buildings

MDPI

Review

A State-of-the-Art Review on the Influence of Porosity on the Compressive Strength of Porous Concrete for Infrastructure Applications

Rajab Abousnina [1,*], Fahad Aljuaydi [2,*], Benchaa Benabed [3], Magdi H. Almabrok [4] and Vanissorn Vimonsatit [5]

[1] School of Civil and Mechanical Engineering, Curtin University, Perth, WA 6102, Australia
[2] Department of Mathematics, College of Sciences & Humanities, Prince Sattam Bin Abdulaziz University, Al-Kharj 11942, Saudi Arabia
[3] Civil Engineering Research Laboratory, Amar Telidji University, Laghouat 03000, Algeria; b.benchaa@lagh-univ.dz
[4] Civil Engineering Department, Faculty of Engineering and Petroleum, University of Benghazi, Benghazi P.O. Box 1308, Libya; magdi.almabrok@uob.edu.ly
[5] School of Engineering, Faculty of Science and Engineering, Macquarie University, Sydney, NSW 2109, Australia; sorn.vimonsatit@mq.edu.au
* Correspondence: rajab.abousnina@curtin.edu.au (R.A.); f.aljuaydi@psau.edu.sa (F.A.)

Abstract

The use of porous concrete in various infrastructure applications such as pavements, infiltration beds, and low-volume load areas is increasingly encouraged due to its environmental benefits. The performance of porous concrete is strongly influenced by its pore structure and overall porosity. Researchers have employed multiple methodologies to characterise pore size and distribution, and to assess their effects on permeability, hydraulic conductivity, and compressive strength. This review investigates several pore measurement techniques aimed at improving both the hydraulic and mechanical performance of porous concrete. Among these, image analysis emerges as the most accurate method for assessing porosity distribution, offering higher resolution and fewer limitations compared to traditional techniques. Despite these advancements, a debate remains regarding the relative importance of effective porosity versus total porosity. This work comprehensively evaluates and synthesises existing methods for pore structure analysis, thereby enhancing our understanding of how porosity influences concrete behaviour. The findings indicate that effective porosity alone is insufficient to predict hydraulic conductivity, whereas total porosity has a considerable effect on compressive strength. This insight can be used to optimise the balance between strength and permeability in porous concrete, supporting its broader implementation as a sustainable construction material.

Keywords: porous concrete; porosity; permeability; infrastructure applications and measurements

check for updates

Received: 22 May 2025
Revised: 4 June 2025
Accepted: 23 June 2025
Published: 1 July 2025

Citation: Abousnina, R.; Aljuaydi, F.; Benabed, B.; Almabrok, M.H.; Vimonsatit, V. A State-of-the-Art Review on the Influence of Porosity on the Compressive Strength of Porous Concrete for Infrastructure Applications. *Buildings* **2025**, *15*, 2311. https://doi.org/10.3390/buildings15132311

Copyright: © 2025 by the authors. Licensee MDPI, Basel, Switzerland. This article is an open access article distributed under the terms and conditions of the Creative Commons Attribution (CC BY) license (https://creativecommons.org/licenses/by/4.0/).

1. Introduction

Porous concrete has become significant appealing in recent decades owing to its capacity to mitigate environmental concerns. It is a type of concrete distinguished by significantly increased water permeability relative to standard-weight concrete [1–3]. Porous concrete is utilised across a wide range of applications, including permeable pavements for stormwater management, base layers for urban roads, rural pathways, driveways, and airport runways. It is also employed in rigid drainage systems beneath open public areas, as a substrate for

vegetation and ecological growth, in thermally insulating concrete, and in various civil and architectural engineering works [4]. Moreover, it is now employed in a variety of applications where sound absorption or thermal insulation are needed [5,6].

Global research and interest in porous concrete have emerged, especially in the United States and Japan. Porous concrete has been employed for over thirty years in both the United States and England [7,8]. A key benefit of porous concrete construction is its capacity to let the percolation of both water and air through an interconnected pore matrix into the underlying subsoil. Many elements, including gradation, aggregate type in the mixture, water amount, cement content, and compaction level, influence the dimensions of these pores [9]. The overall vacancy percentage in porous concrete can range from 10% to 40% [10–12]. Moreover, permeability is a key performance characteristic of porous concrete. As with any permeable material, its transport properties are fundamentally influenced by the characteristics of its pore structure [13]. However, permeability in porous concrete is often associated with its porosity, mainly due to the simplicity of measuring porosity in such a macro-porous material. Unlike conventional concrete, permeable concrete is characterised by its high porosity, which is essential for ensuring interconnected pores and facilitating fluid flow [14,15]. Conversely, the compressive, tensile, and flexural strength of porous concrete mixtures is often inferior to that of conventional concrete, attributable to the elevated void ratio and absence of fine aggregate. The elevated permeability of porous concrete enables a substantial reduction in stormwater runoff; as a result, it is considered an effective approach within stormwater management best practices [16]. Nevertheless, when the vacancy percentage escalates, the strength of the cured concrete often diminishes [17,18]. The decrease in strength would undoubtedly impact the characteristics of the porous concrete; therefore, additional inquiry into the optimal correlation between the features of porous concrete to obtain maximum efficiency in both strength and permeability is necessary. Essential data have been analysed concerning how the void ratio, the water-to-cement (w/c) ratio, cement paste properties, the proportion and size of coarse aggregates, and overall strength influence porous concrete performance [3,16,19–21]. Further exploration into the impact of pore structure on the permeability, hydraulic conductivity, and compressive strength of porous concrete is necessary to attain optimal strength and durability at the specified void ratio.

2. Properties of Porous Concrete

2.1. Workability

Numerous practitioners of porous concrete have encountered situations where applying classic concrete concepts to porous concrete has yielded a suboptimal final product. To date, determining how workable porous concrete is has been seen as an art, since the usual slump test does not give helpful information for this hard concrete. While several studies have documented slump tests for porous concrete, the conventional slump test is inadequate for evaluating its workability due to its low density [16,22–26]. It is advised that the workability of porous concrete be evaluated by shaping a ball with the hand to determine its mouldability [27,28]. The mouldability of porous concrete is highly sensitive to water content; therefore, the water quantity must be meticulously regulated. However, Kevern, et al. [29] have stated that this method is impossible to specify due to the lack of quantifiable values and individual bias. In their research, a Superpave Gyratory Compactor (SGC) was altered to provide a testing methodology for characterising the workability of porous concrete. This approach generated porous concrete samples utilising an SGC that replicates diverse field compaction conditions. The link between density and gyration subsequently determined the workability of the concrete. A matrix of concrete mixes with varying water-to-cement ratios and cement concentrations was evaluated. The

impact of mixing duration on concrete workability was assessed to determine the "slump loss" of field porous concrete. The results indicated that the SGC consistently generated porous concrete specimens, and the test procedure effectively assessed the workability and compatibility of the plastic concrete. The capacity to accurately delineate this method is constrained by the absence of quantifiable indicators and the possibility of human bias. Researchers have modified a Superpave Gyratory Compactor (SGC) to provide a standardised testing protocol for assessing the workability of porous concrete. This technique entails the fabrication of porous concrete specimens via an SGC, which replicates diverse field compaction scenarios. The workability is evaluated by examining the correlation between density and gyration. A variety of concrete mixtures with varying water-to-cement ratios and cement concentrations were evaluated, and the influence of the mixing period on workability was analysed to ascertain the "slump loss" of field porous concrete. The results indicated that the SGC efficiently generated consistent porous concrete specimens, and the testing methodology accurately assessed the workability and compatibility of plastic concrete [30,31].

2.2. Density

The density of porous concrete is determined by both the characteristics and ratios of its components, along with the compaction methods applied during placement. Its increased porosity distinguishes it from other lightweight materials. The density of porous concrete ranges from 1500 kg/m^3 to 2200 kg/m^3 [32–35]. Therefore, a pavement with a thickness of 125 millimetres and a void percentage of twenty percent can retain twenty-five millimetres of water throughout a continuous thunderstorm within its voids. When placed on top of a 150 mm thick layer of open-graded gravel or crushed rock sub-base, the storage capacity increases to 75 mm of precipitation at that level [36–38]. The density of porous concrete is significantly influenced by the aggregate usage rates and grain size distribution. Increasing the volume of coarse aggregates generally increases the density by reducing the overall porosity, whereas using finer aggregates tends to fill voids more effectively, resulting in a denser and stronger matrix. Conversely, larger aggregate sizes promote higher porosity and lower density, which enhances permeability but may reduce compressive strength [3,39,40]. Optimising the balance between aggregate content and grain size is therefore critical to tailoring the density and performance of porous concrete for specific applications.

2.3. Compressive Strength of Porous Concrete

Porous concrete generally exhibits much lower compressive strength compared to conventional Portland cement concretes with similar water-to-cement ratios. The mixture proportions and compaction process significantly affect the flexural and compressive strength of porous concrete. Consequently, as the void content escalates, the compressive strength of porous concrete diminishes; hence, porous concrete exhibits inferior strength compared to conventional concrete. The mean compressive strength of porous concrete is approximately 20 MPa, with a minimum value of 2.0 MPa and a maximum strength of 34.5 MPa documented [27,41,42]. Highly porous concrete has a compressive strength of half or one-third that of regular concrete. Nevertheless, void space and, consequently, the percolation rate through the material must be sacrificed to achieve higher porous concrete strengths. Several parameters determine the strength of porous concrete. These factors include the type of binder, the type of aggregate, the aggregate grading, the mix composition, and the consistency of the concrete [41,43–46]. The primary characteristics associated with these metrics are the workability, density, cement binder, and pore structure of the material.

2.4. Permeability

Porous concrete is distinguished by its high permeability, which is the most noticeable feature of this material. This characteristic refers to water transport via pore spaces, which depends on the materials, mixes, compaction, and placement procedures carried out. The capillary pores inside the cement paste determine permeability. Low permeability results from pores that are too small, while high permeability results from massive holes. Hydraulic conductivity (K) is the term that is used to refer to permeability in a formal sense. The key parameter utilised in the hydrological design of porous concrete is the material's permeability.

Darcy's Law and the assumption of laminar flow inside porous concrete are the two fundamental principles upon which most permeability measurements are based. Equation (1) can be used to determine the coefficient of permeability.

$$K = \frac{A_1 L}{A_2 t} ln\left(\frac{h_2}{h_1}\right) \tag{1}$$

In this context, A_1 and A_2 represent the cross-sectional areas of the specimen and the tube, respectively, while L denotes the length of the sample. For a fixed specimen geometry, h_1 and h_2 correspond to the initial and final water heads, and t is the time required for the water level to drop from h_1 to h_2.

Figure 1 illustrates the relationship between permeability, porosity, and pore structure characteristics, which was derived using the Kozeny–Carman equation in conjunction with Darcy's law and pore geometry considerations, as presented in Equation (2).

$$K = \frac{\varnothing_t^3}{C_o\{L_e/l\}_0^2(1-\varnothing)^2 SSA_s^2} \frac{\gamma}{\mu} \tag{2}$$

where pore tortuosity $(L_e/l)o$, the specific surface area (SSA) and total porosity ($\varnothing_t$) of CPP are key parameters, while the shape factor (C_o), which reflects pore geometry, typically ranges from 2 to 3—depending on whether the pores are assumed to be circular or rectangular. For filter media with a mixed pore distribution, a value of 2.5 is commonly used, where μ is dynamic viscosity.

According to [47], hydraulic conductivity can be related to intrinsic permeability as follows:

$$\mathrm{K} = \mathrm{k}\,\frac{\rho g}{\mu} \tag{3}$$

where ρ = density of the fluid, and g = acceleration due to gravity. Intrinsic permeability (k) is influenced by factors such as the material's porosity, the distribution and roughness of its pores, the narrowness of pore pathways, and the complexity and connectivity of internal pore networks.

Intrinsic permeability can be described by simplifying Equation (4) as follows:

$$k = \frac{\varnothing^3}{F_s\ \tau^2\ \ S_0^2(1-\varnothing)^2} \tag{4}$$

where F_s represents the generalised factor accounting for various pore geometries, τ denotes the tortuosity of the pore pathways, So refers to the specific surface area, and $\varnothing$ is the porosity.

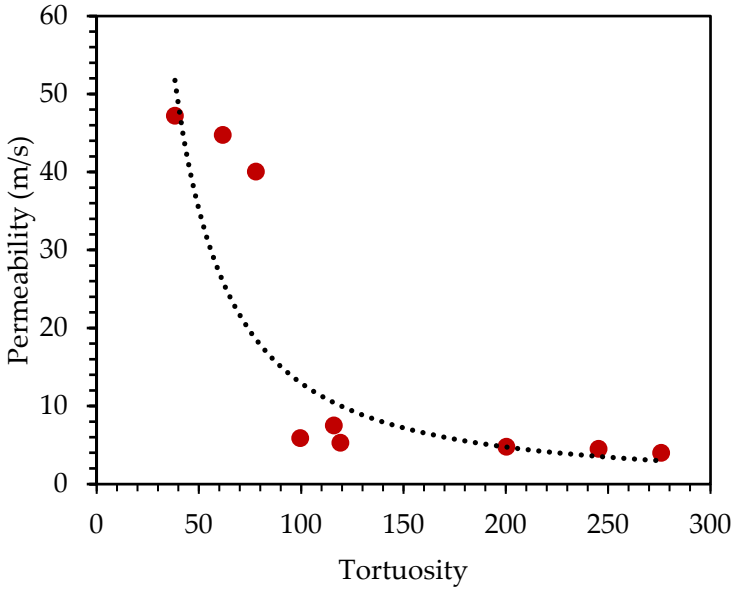


Figure 1. Variation in permeability with pore structure features (re-plotted by the authors based on data from [48]).

2.5. Conductivity

A porous concrete's hydraulic conductivity (K) is based on the pores and their relative sizes. Due to the intricately interwoven pore structure of porous concrete, conventional methods for evaluating the hydraulic conductivity of normal concrete are not immediately applicable [41,49]. The intrinsic permeability (k) of porous concrete indicates the frictional resistance encountered by a fluid traversing through it. Consequently, intrinsic permeability is contingent upon porosity, pore-size distribution, pore roughness, constrictions inside the pore space, and the tortuosity and connectedness of the internal pore channels [50,51]. The hydraulic conductivity can be related to intrinsic permeability as follows:

$$K = k\frac{\rho g}{\mu} \tag{5}$$

where ρ represents the fluid's density, g denotes the acceleration due to gravity, and μ signifies the dynamic viscosity of the fluid. This equation may be simplified for water as follows:

$$K = k * 10^7 \tag{6}$$

The intrinsic permeability of porous concrete is commonly characterised using the Kozeny–Carman equation:

$$k = \frac{\varnothing_p^3}{F_s \tau^2 S_0^2 (1 - \varnothing_p)^2} \tag{7}$$

where ϕ_p denotes porosity, F_s represents the generalised factor for varying pore geometries, τ signifies tortuosity, and S_0 indicates the particular surface area of the pores.

Another investigation established a correlation between pore volume and conductivity [52]. The hydraulic conductivity of the porous concrete was determined via a falling head permeability cell. The permeability coefficient (K) was determined by Darcy's law as follows:

$$K = \frac{A_1 l}{A_2 l} log\left(\frac{h_2}{h_1}\right) \tag{8}$$

A_1 and A_2 denote the areas of the sample and tube cross-section, respectively, whereas l represents the length of the specimen. For a certain specimen geometry with identical beginning and final heads, the coefficient of permeability is expressed as follows:

$$K = \frac{A}{t} \tag{9}$$

A is a constant, namely, 0.084 m, in this investigation. The hydraulic conductivity values recorded varied from 0.001 to 0.005 m/s, with a standard deviation ranging from 0.0003 to 0.0008 m/s across three repeated experiments. As shown in Figure 2, a comparison is made between the effective conductivities predicted by Archie's law and those obtained from experimental data [53].

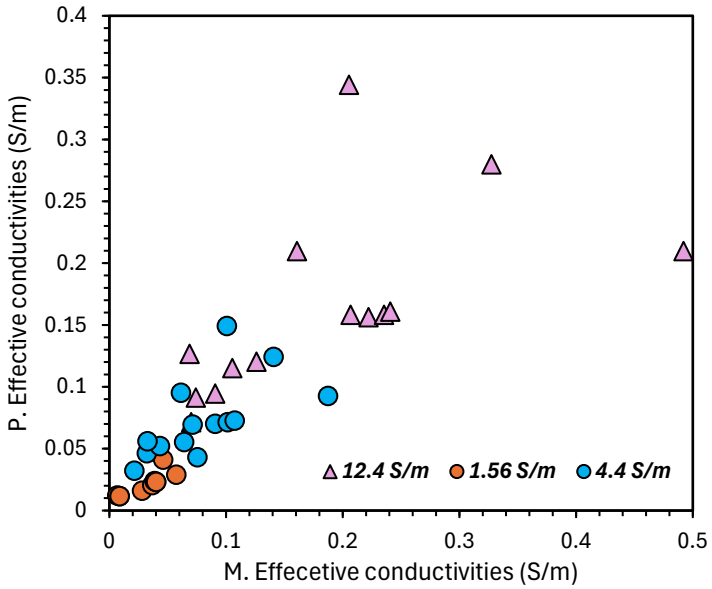


Figure 2. The comparison between effective conductivities predicted using the conventional Archie's law and those obtained from experimental measurements [53].

Based on the previous subsections, the porosity, pore structure, and pore size are the most effective parameters for strength, permeability, and hydraulic conductivity.

2.6. Elastic Modulus

An essential characteristic used in constructing porous concrete pavements is known as the modulus of elasticity [54]. Comprehending the behaviour of the elastic modulus concerning aggregate proportions and characteristics can enhance the input parameters for porous concrete design. Various aggregate sizes allow smaller particles to fill the interstices between bigger ones, reducing vacant space and minimising paste needs. Simultaneously, bigger maximum aggregate sizes might decrease void space, despite the comparatively greater median void size [55]. Porous concrete may be comprehended similarly. Nonetheless, porous concrete is engineered to have sufficient paste to cover the aggregates without an excess that would occupy the voids. Examining the differences in aggregate gradation, quantity, and dimensions can enhance comprehension of the paste needs for porous concrete. According to the findings of specific studies, the coarse aggregate is the key factor determining the elastic modulus values in an ordinary concrete mixture [56]. Aggregate stiffness, type, volumetric content, and size are some elements that affect the modulus of elasticity of concrete with normal strength [57,58]. Typically, a rise in the compressive strength of concrete correlates with an increase in the elastic modulus [59,60]. At constant aggregate content, using smaller aggregate sizes leads to increased compressive strength,

whereas larger aggregate sizes tend to enhance the elastic modulus [61]. Concrete mixtures with greater proportions of coarse aggregate tend to exhibit slightly elevated elastic moduli, as aggregates are the most rigid component, and increasing their content enhances the overall stiffness of the material [62]. Research conducted by Haselbach and Alam [63] estimated the modulus of elasticity of porous concrete based on porosity. The elastic modulus for 20% porosity in porous concrete varies from 14 to 22% at 2.2 MPa stress and 24 to 32% at 2.8 MPa stress. Reduced aggregate sizes provide increased compressive strengths at equivalent aggregate volumes. Conversely, the elastic modulus rises with higher aggregate sizes [64,65]. Moreover, concretes with elevated coarse aggregate concentrations show marginally increased elastic moduli. Aggregates are the most rigid component in conventional concrete; hence, increasing the quantity of aggregate yields a stiffer final product [56,66]. The correlation between the modulus of elasticity and porosity in porous concrete indicates that at 20% porosity, the elastic modulus varies from 14% to 22% at a tensile stress of 2.2 MPa and from 24% to 32% at a stress level of 2.8 MPa [67].

2.7. Porosity

Several elements, including binder kinds, aggregate types, aggregate grading, mix composition, and compaction, influence the strength and porosity of porous concrete [41,68–71]. The porosity of porous concrete varies between 15% and 30%. The porosity of porous concrete is referred to as void content or void ratio expressed as a percentage. The elevated porosity increases porous concrete's permeability [72–75]. The significance of void content in porous concrete is paramount. Excessive void content diminishes strength, while insufficient void and permeability render the concrete hardly porous. The practical design of porous concrete relies significantly on achieving an optimal equilibrium between strength and porosity. The extensive interconnecting voids in the material are achieved using a nearly uniform aggregate of comparatively big grains. The arrangement of this coarse aggregate results in significant voids because of the uniformity in grain sizes. Different amounts of voids in finished concrete depend on how much binder is allowed to mix with the particles [76].

The adhesion between aggregates coated with a cementitious matrix has been analysed, revealing that the bonding force among the aggregates is primarily influenced by the contact area (aggregate size) and the tensile strength of the matrix. The compressive strength of porous concrete offers a rapid evaluation of the bond strengths between gap-graded particles and the influence of its porosity. The contact area can be increased by utilising smaller particles. Altering the aggregate size and the aggregate-to-binder ratio can substantially influence porosity. It is well accepted that an increase in porosity reduces compressive strength. Figure 3 depicts a schematic of porous concrete. The porous concrete has substantial voids, unlike conventional concrete, which includes small cavities [76–78].

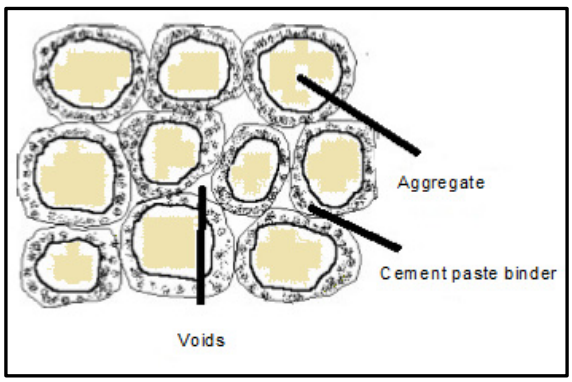


Figure 3. A schematic diagram of porous concrete [79].

2.7.1. Pore Structure

Porous concrete consists of three main types of pores: gel pores in the cement paste, voids between aggregates, and air voids, as illustrated in Figure 4. Gel pores are smaller than capillary pores, whose presence is influenced by the water-to-cement ratio and the age of the concrete. These pores may be isolated or interconnected. Air voids, typically larger, often contribute to water permeability and are primarily affected by aggregate grading and compaction levels. Aggregate voids vary in size and connectivity, depending on the type of aggregate used. These pore types are either interconnected or exist independently. The interconnected air gaps may enhance the material's water permeability. The aggregate grade and compaction degree are the main elements that affect this. The types of aggregate used may cause differences in aggregate void sizes, which may or may not be connected. Figure 4 shows the types of pores of porous concrete.

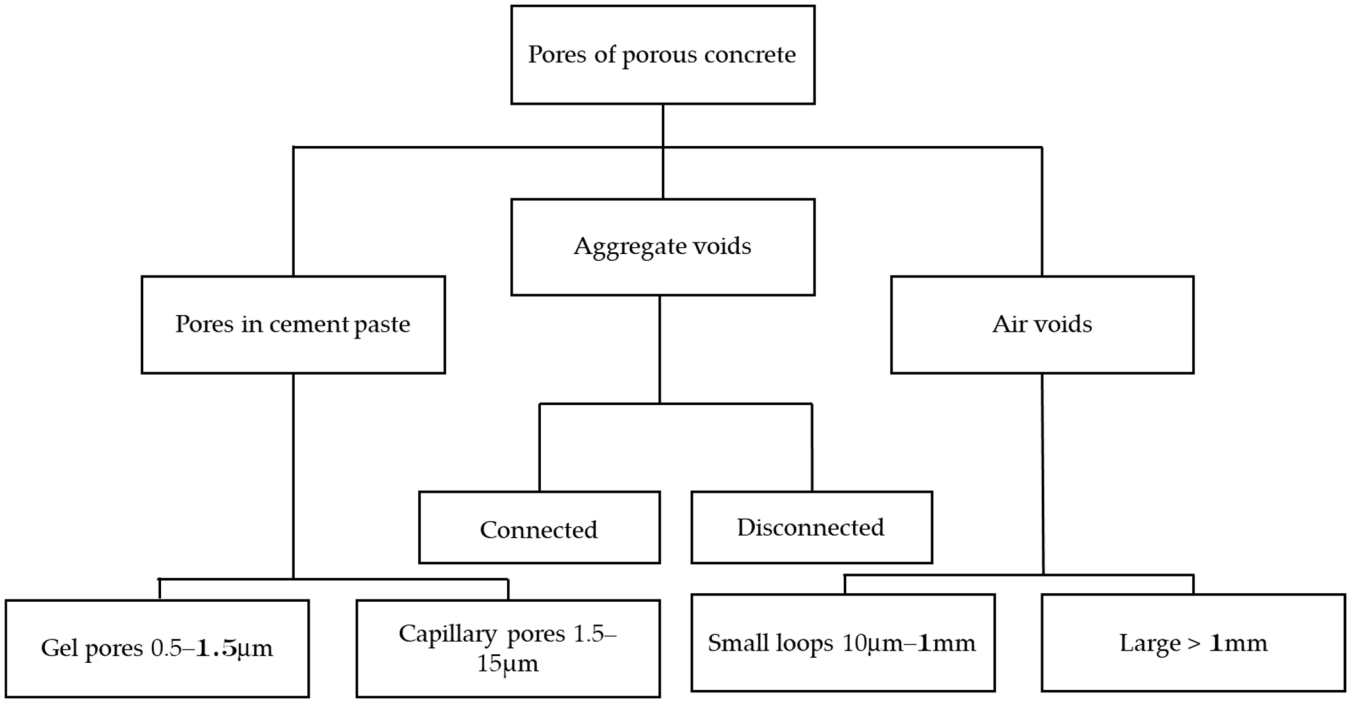


Figure 4. Types of pores of porous concrete.

Porosity is determined using the water displacement method proposed by Montes, et al. [80], based on Archimedes' principle of buoyancy, which states that the buoyant force acting on an object is equal to the weight of the fluid it displaces. This method enables the calculation of total porosity, as presented in Equation (10).

$$P = \left[1 - \left(\frac{M_{dry} - M_{sub}}{\rho_w * V_T}\right)\right] 100\% \quad (10)$$

where P is the porosity of the sample, M_{dry} and M_{sub} are the dry and submerged mass of samples, respectively, and ρ_w and V_T are the density of water and the total volume of the sample, respectively.

The total volume is found by measuring the height and the diameter of the samples at three different locations, and the average is calculated using Equation (11).

$$V_T = \left(D_{avg}\right)^2 \times \pi \times \frac{H_{avg}}{4} \quad (11)$$

V_T is the total volume of the sample, D_{avg} is the diameter of the cylindrical sample, and H_{avg} is the average height of the sample.

The dry mass is determined by baking the sample in an oven at 110 °C for 24 h, as per the guidelines established by Montes, et al. [80]. To determine the submerged mass, the sample is placed in water for at least 30 min, allowing for sufficient time for water to penetrate all interconnected pores. While still submerged, the specimen is gently tapped against the side of the container to release any trapped air bubbles. The submerged weight is then measured using a digital scale with the sample held in a wire mesh basket.

2.7.2. Effective Porosity

The segment of total pore space engaged in specific operations is called "effective porosity." The effective porosity fluctuates depending on the procedure under consideration. In fluid flow and drainage, efficient porosity omits solitary holes, dead-ended pores, and capillary pores. Dead-ended and capillary holes are included for fluid retention. Consequently, a clear definition must be established to characterise "effective porosity objectively." Researchers categorise effective porosity as the proportion of total porosity in a porous concrete specimen that has drained for 30 min, and they also define "rapid flow" porosity; nevertheless, they advise against the use of this "effective porosity" owing to heightened variability [81,82]. Kalman and Portnikov [83] stated that the void ratio was utilised in their computations, defined as the volume of voids divided by the volume of solids. This ratio was determined following the ASTM Standard Test Method for Bulk Density ("Unit Weight") and Voids in Aggregate (C29/C29M–97), combined with an estimated specific gravity of the cement-paste-coated aggregate mixture. In this study, the focus is on calculating total porosity, given the variability in how effective porosity is defined across different methodologies. Due to the elevated void volume, typical fraction tests, such as ASTM C173 [84], are not suitable for directly assessing the porosity of porous concrete. Consequently, the porosity was determined by calculating the weight difference between oven-dried and water-saturated samples. Equation (12) was used to estimate the effective porosity:

$$\varnothing_e = \left[1 - \left(\frac{M_1 + M_2 - M_3}{\rho_w V_T}\right)\right] \times 100\% \quad (12)$$

$\varnothing_e$ is the effective porosity.
M_1 is the mass of the oven-dried sample.
M_2 is the mass of the container filled with water.
M_3 is the container with saturated sample filled with water at the same level.
ρ_w is the density of water.
V_T is the volume of the sample.

2.7.3. Effective Porosity Versus Total Porosity

The specified method quantifies the volume of accessible pores (V_{ap}). The total volume (V) is composed of the total pore volume (V_p), the volume of the aggregate (V_{agg}), and the volume of the matrix (V_m). Effective porosity ($\varnothing_e$) is defined as the ratio of Vap to the total volume (V) and plays a vital role in determining the hydraulic conductivity of porous concrete. While many researchers associate effective porosity with compressive strength, it is the total porosity that more directly influences this property. Total porosity ($\varnothing_t$) is defined as the ratio of total pore volume (V_p) to total volume (V), as expressed in Equation (13). Total porosity considers the volume of non-accessible pores (V_{nap}). The volume of non-accessible pores may be categorised as non-connected pores situated between aggregates (V_{ncp}) and the pores inside the matrix (V_{mp}). Figure 5 illustrates the pore structure in porous concrete. To determine the volume of accessible pores (V_{ap}), several methods can be used,

including water saturation tests, mercury intrusion porosimetry (MIP), and image analysis, which help identify interconnected and open pores. For the volume of non-accessible pores (V_{nap}), MIP and X-ray computed tomography (CT) can be employed, while an indirect estimation approach can be applied by subtracting Vap from the total pore volume (V_p).

$$\varnothing_t = \frac{V_p}{V} = 1 - \frac{\rho}{\rho_t} \tag{13}$$

$$\rho = \frac{M}{V} \tag{14}$$

where Vp is the pore system's total volume, V and q are the bulk volume and density, respectively, and ρt is the density of the void-free porous concrete, which can be calculated using the following equation.

$$\rho_t = \frac{m_{agg} + m_m}{V_{agg} + V_m - \Delta V_m} = \frac{M}{V_{agg} + V_m - \Delta V_m} = \frac{\left(1 + \frac{A}{B}\right) * m_m}{V_{agg} + V_m - \Delta V_m} = \frac{\left(1 + \frac{A}{B}\right) * m_m}{V_{agg} + \left(1 - \frac{\Delta V_m}{V_m}\right) * V_m} \tag{15}$$

$$V_{agg} = \frac{m_{agg}}{\rho_{agg}} \tag{16}$$

$$V_m = \frac{m_m}{\rho_m} = \frac{m_w}{\rho_w} + \frac{m_c}{\rho_c} + \frac{m_{SF}}{\rho_{SF}} + \frac{m_{GP}}{\rho_{GP}} \tag{17}$$

where m_{agg}, m_m, m_w, m_c, m_{SF} and m_{GP} are the weight of aggregate, matrix, water, cement, silica fume, and glass powder, respectively, V_{agg} and V_m are the dry volume of the aggregate and matrix, respectively, and ΔV_m is the matrix volume reduction after hydration, and ρ_{agg}, ρ_w, ρ_c, ρ_{SF}, ρ_{GP} are the density of aggregate, water, cement, silica fume, and glass powder, respectively. Research has shown that after hydration, matrix volume reduction is 25% of the volume of non-evaporable water (V_{new}). The weight of non-evaporable water is about 23% of anhydrous cement based on the assumption that cement is fully hydrated [85]. Based on this, the value of ΔV_m is calculated as follows:

$$\Delta V_m = 25\% \times V_{new} = 25\% \times 23\% \times \frac{m_c}{\rho_w} \tag{18}$$

where V_{new} is the volume of non-evaporable water, m_c is the mass of anhydrous cement, which will be fully hydrated, and ρ_w is the density of water.

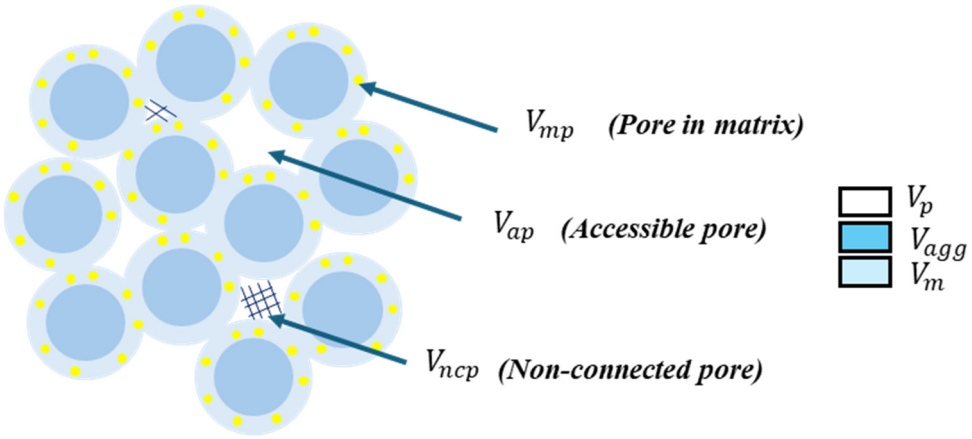


Figure 5. Pore system of porous concrete created based on the design and information from [77].

3. Factors Affecting the Porous Concrete

3.1. Cement Binder

The cement binder is a crucial component of porous concrete. The durability of hardened porous concrete is contingent upon the strength of the cement paste binder. The cured cement paste binder's strength is compromised due to its thinness, and the existence of pores and microcracks in the hardened cement binder substantially influences its strength [86]. Voids constitute a vulnerability in a cement matrix, leading to fracture development [75,78,87]. The cement paste binder is crucial in porous concrete. A multitude of investigations have been undertaken with diverse cement compositions. Table 1 presents a prior investigation conducted by different researchers. Analysis of the table indicates that an increase in cement content correlates with an enhancement in the compressive strength of cured porous concrete. To validate the findings of the preceding research shown in Table 1, the authors performed a straightforward investigation using various kinds of cement content. Table 1 presents the study's findings, indicating that increased cement content generally enhances the strength of hardened porous concrete.

Table 1. Previous studies on a variety of cement content types in a porous concrete mix.

Aggregate (kg/m^3)	W/C Ratio	Cement (kg/m^3)	Compressive Strength (MPa)	References
1800	0.35	250	3.45	[88]
1600	0.35	200	2.80	
1800	0.35	150	1.83	
1263	0.32	554	19.89	[89]
1279	0.33	496	14.65	
1286	0.33	411	9.66	
1560	0.3	367	13.9	[90]
1560	0.3	242	8.6	
1115	0.34	450	18.03	[91]
1450	0.33	440	14.37	
1430	0.33	400	11.82	

Various scholars have undertaken prior research to enhance the strength of hardened cement paste. In the absence of adjustments, it is challenging to produce high-strength concrete [92]. The use of superplasticisers significantly decreased the water-to-cement ratio, thereby enhancing the strength of the paste, which is highly beneficial [93,94]. Moreover, the amalgamation of SP and a cohesive agent might provide favourable workability and strength characteristics [95]. The addition of polymers to the mixture often increases both the compressive and flexural strengths of the material. Furthermore, the incorporation and/or substitution of silica fume [96] and nano-silica [97] in the cement's composition enhances the strength of the cured cement paste.

3.2. Aggregates

The aggregate size used in porous concrete varies from 19 to 9.5 mm to provide enough voids within the material [72,98]. Nonetheless, some researchers used coarse aggregates ranging from 9.5 to 2.36 mm to enhance strength [99–103]. Table 1 displays the standard aggregate compositions used in various investigations. The aggregates used in porous concrete should possess attributes as delineated in [32], which outlines specification limitations for characteristics influencing the performance of porous concrete pavements [104,105]. The thresholds for harmful substances, including clay and

chert, are specified since they influence the adhesion between aggregate and cement paste. The physical parameters of aggregates used for porous concrete must resemble those utilised in conventional concrete. The collective physical attributes, including dimensions, form, and distribution, significantly influence porous concrete pavements' mechanical, durability, and permeability properties [106,107]. In addition to the overall size, the kind of aggregate significantly affects the characteristics of porous concrete. While limestone aggregate is often used for porous concrete production, many investigations have shown that dolomitic aggregates provide superior compressive strength at elevated porosity levels compared to analogous combinations using limestone/slag aggregates [108,109]. Research conducted by [110] used aggregate types from seventeen sources to examine the impact of aggregates on freeze–thaw (F-T) resistance. The porous concrete mixes composed of granite aggregate demonstrated enhanced freeze–thaw resistance regardless of source or location. The mixes of limestone and river gravel aggregates were readily compromised by freeze–thaw cycles. The physical features of aggregates, including abrasion resistance and water absorption, significantly influenced the mitigation of F–T damage. The findings suggested that the characteristics of aggregates must be regulated in porous concrete due to the thin cement paste, which facilitates water infiltration into the pores of individual aggregates, hence increasing the likelihood of freeze–thaw damage and durability cracking in these pavements.

3.3. Admixtures

Porous concrete often exhibits minimal slump, necessitating various admixtures to enhance workability without excessive water content augmentation. Numerous studies have used water-reducing admixtures to enhance workability, and ACI 522R [111] also recommends utilising several kinds of admixtures. Retardation admixtures might facilitate field installation challenges since porous concrete may need extended time for placement and finishing due to its rigidity. Furthermore, evaporation retarders are advised to minimise the evaporation of gauged water from the newly applied surface, while air-entraining admixtures may be used to enhance freeze–thaw durability.

3.4. Mix Design

Research papers advocate diverse mix designs and proportioning techniques for porous concrete based on various concepts [112–115]. The fundamental idea of mix design is to provide sufficient cement coverage on the aggregates. Nguyen, et al. [112] formulated a porous concrete mix design and proportioning hypothesis based on the excess paste theory. The amount of cement paste necessary for adequate coating was calculated by dividing it by the surface area of the spherical aggregates. In another study, the conventional technique for determining mix proportions for porous concrete was based on the absolute volume approach. At the same time, a mix-proportioning technique using the ratio of paste volume (PV) to inter-particle voids (IPVs) was also introduced [116,117]. Table 2 presents the mix proportions used by different researchers in their studies and designs. The overall density content ranged from 1400 to 1800 kg/m^3, with an aggregate-to-cement ratio of 4:1 to 12:1. The water-to-cement ratio ranged from 0.2 to 0.42, lower than that of traditional concrete.

Table 2. The mix proportions used by different researchers in their studies and designs.

Aggregate, kg/m^3	Cement Material, kg/m^3	Water kg/m^3	A/C Ratio	w/c Ratio	Reference
1651.32	412.83	153.57	4:1	0.372	[118]
1692	376	143.25	4.5:1	0.381	
1740	348	135.72	5:1	0.390	
1800	300	125.4	6:1	0.418	

Table 2. *Cont.*

Aggregate, kg/m^3	Cement Material, kg/m^3	Water kg/m^3	A/C Ratio	w/c Ratio	Reference
1541.93	344.69	105.01	4.47:1	0.3	[119]
1620.24	287.15	87.21	5.46:1	0.3	
1820	180	50	10:1	0.28	[29]
1700	260	70	6.5:1	0.27	
1620	310	80	5.2:1	0.26	
1580	330	90	4.78:1	0.27	
1550	360	100	4.3:1	0.28	
1510	380	100	3.97:1	0.26	
1600	340	80	4.70:1	0.24	
1570	330	100	4.75:1	0.30	
1560	330	100	4.72:1	0.30	
1440.8	320.2	112.1	4.5:1	0.35	[120]
1486.9	330.4	115.6	4.5:1	0.35	
1586.9	352.6	123.4	4.5:1	0.35	
1559	312	103	5:1	0.33	[47]
1568	314	104	5:1	0.33	
1558	312	103	5:1	0.33	
1524	305	101	5:1	0.33	
1546	309	102	5:1	0.33	
1544	309	102	5:1	0.33	
1560	367	110.1	4.25:1	0.30	[121]
1560	242	72.96	6.44:1	0.30	
1560	367	73.4	4.25:1	0.20	
1560	367	110.1	4.25:1	0.30	
1560	430	110.1	3.62:1	0.26	
1560	495	148.5	3.15:1	0.30	
1600	200	70	8:1	0.35	[88]
1800	150	52.85	12:1	0.35	

3.5. W/C Proportion

In porous concrete, water-to-cement ratios typically range from 0.27 to 0.30 with the appropriate use of chemical admixtures, although ratios as high as 0.34 and 0.40 have also been successfully applied. The relationship between strength and the water-to-cement ratio remains unclear in porous concrete, as the total paste content is lower than the void content within the aggregate structure, unlike in conventional concrete [3]. Increasing the paste's strength may not necessarily result in an overall increase in strength. Water content must be meticulously regulated. The appropriate water concentration is characterised by imparting a shine to the mixture without causing it to drip off the aggregate. A small quantity of porous concrete shaped into a sphere will maintain its integrity and void structure as the paste permeates the interstices among the particles.

4. Measurement of Porosity

The pore space in porous concrete is seldom uniform; so, pore size may be characterised using stereological or morphology-based approaches in random porous media [122]. Consequently, many techniques have been used to assess porosity. Porosity was measured by incrementally adding a specified volume of water to a vessel holding a suspended porous material. The relationship between the volume of water added and the change in water level enabled the calculation of porosity values at various heights along the specimen. Nonetheless, other challenges associated with this method were recognised, including the capillary action of water, which increased water absorption by the sample, amplifying its perceived porosity at that site.

Furthermore, when the sample is further submerged, some voids may entrap air, which might be released during other porosity-testing methods, thus resulting in diminished apparent porosity levels [123–125]. This issue would be intensified when porosity is less. The modest compaction resulting from surface smoothing led to a consistent pattern in the findings for the nine examined samples, indicating a marginally reduced porosity at the surface. This was ascribed to the compaction technique used, namely, the "vibration compaction method." The vibration induced the lower-viscosity cement paste to descend to the sample's base, augmenting the higher porosity while diminishing the lower one [126–129]. The pore structure in porous concrete is seldom uniform; so, pore size may be characterised using stereological or mathematical morphology approaches in random porous media [130,131]. Consequently, many techniques have been used to quantify porosity. Bustillo Revuelta and Bustillo Revuelta [132] assessed porosity by progressively introducing a predetermined amount of water into a suspended porous specimen container. The correlation between the amount of water introduced and the alteration in water level facilitated the determination of porosity values at incremental heights along the specimen. Nonetheless, several difficulties with this strategy were identified and documented, including the capillary movement of water, which caused the sample to absorb more water, creating an illusion of increased porosity at that location [133,134].

4.1. InstroTek-Based Corelok Sealing Technique

The InstroTek Corelok System differs from earlier porosity measurement techniques by using a vacuum to aid in air removal and water infiltration into the porous matrix. The procedure involves enclosing the sample in an impermeable polymer bag and employing a vacuum pump to evacuate air from its internal structure. Once vacuum-sealed, the specimen's mass is measured while submerged in water. While underwater, the bag is unzipped, allowing water to enter both the bag and the porous sample. The submerged mass is then recorded, and porosity is calculated using the water displacement method. The vacuum environment within the polymer bag minimises retained air, enabling quicker water penetration compared to standard submersion tests [135]. This approach was adapted based on the AASHTO Standard Test Method for Bulk Specific Gravity of Compacted Bituminous Mixtures Using Saturated Surface-Dry Specimens (T 166), which typically shows a variation of 2–4% [136,137]. The T 166 method determines the theoretical maximum specific gravity of a mixture; however, it is not recommended for specimens that absorb more than 2% of their mass in water when submerged.

4.2. Weight Differentiation Method

Several studies [32,138–140] used a distinct approach for measuring total porosity. The open porosity was quantified as the fraction of pore volume or space in concrete capable of holding water. All samples were desiccated at 110 °C. The sample's dimensions were assessed under dry circumstances, and the total volume of the sample (V_T), including both solid and void components, was ascertained. The sample was submerged in a bucket containing enough water to completely cover it, and the water level was recorded. After 24 h, the sample was removed from the bucket, and the water was replenished to the designated level. The scale recorded the weight of the added water, which corresponded to the altered volume (V_C). The equation used was the following:

$$P\ (\%) = \frac{V_T - V_C}{V_T} \times 100\% \tag{19}$$

where P is the open porosity (%), V_T is the total volume of the specimen (mm^3), and "$V_T - V_C$" is the volume of void space (mm^3).

4.3. Japan Concrete Institute (JCI) Method

Safiuddin and Hearn [141] demonstrated that vacuum saturation resulted in the highest permeable porosity. Matsuo, et al. [142] assessed the total and continuous air void content in porous concrete using the experimental procedure recommended by the Japan Concrete Institute (JCI). Two approaches are available for calculating total porosity: one based on volume and the other on mass. The void content determined using the volume-based method is presented in Equation (20), and the linear relationship between total and continuous porosity is illustrated in Figure 6.

$$A_t = 1 - \frac{M_2 - M_1/\rho_w}{V_1} \times 100 \quad (20)$$

where A_t = total air void content of porous concrete.

M_1 = buoyant mass of the saturated specimens in water.

M_2 = dry mass in the air for 24 h.

V_1 = total volume of specimens.

ρ_w = density of water.

The void content based on mass is the methodology given by Equation (21).

$$A_t = \frac{T - W}{T} \times 100 \quad (21)$$

where A_t = total air void content of porous concrete.

T = mass of unit volume in the assumption of no air.

W = mass of unit volume in the container.

The mass of unit volume in the assumption of no air (T) is given by Equation (22):

$$T = \frac{W_4}{V_2} \quad (22)$$

where W_4 = total mass of all materials on the concrete of 1 m^3.

V_2 = sum of the absolute volume of all materials in the concrete of 1 m^3.

In this equation, absolute volume means each mass of every material is divided by density.

The mass of the unit volume in the container (W) is calculated by Equation (23).

$$W = \frac{W_3}{V_1} \quad (23)$$

where W_3 = mass in the air after 24 h.

V_1= total volume of specimen.

There is one methodology given by JCI [143] to determine the continuous air void content of porous concrete and this is given by Equation (24)

$$A_c = \frac{M_1 - M_3/\rho_w}{V_1} \times 100 \quad (24)$$

where A_c = continuous air void content.

A_t = total air void content of porous concrete.

M_1 = buoyant mass of the saturated specimens in water.

M_3 = buoyant mass of the saturated specimens in water after 24 h drying in the air.

V_1 = total volume of specimens.

ρ_w = density of water.

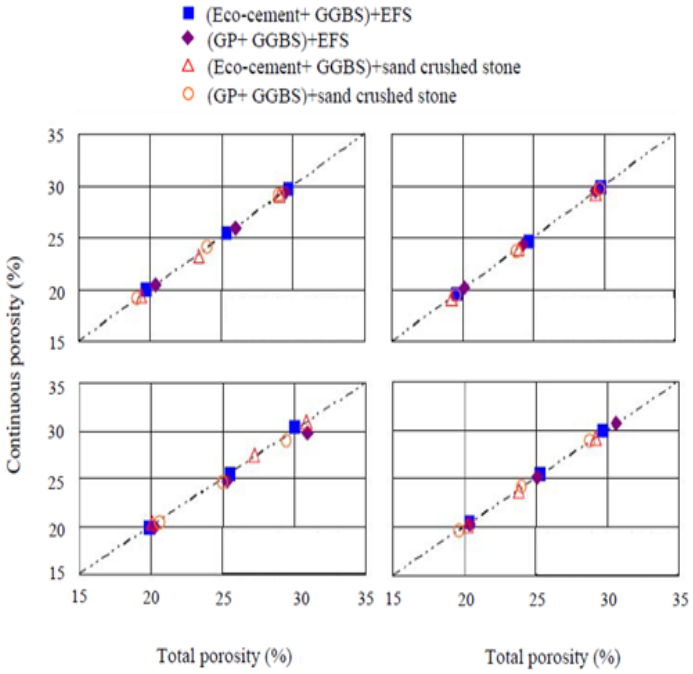


Figure 6. Linear relationships between total porosity and continuous porosity [142].

4.4. Theoretical Method

The NIST hardcore/soft shell (HCSS) model depicts the virtual microstructure of porous concrete, as seen in Figure 7. This model depicts three-phase materials: rigid core spherical particles, a pliable shell, and a bulk phase. This depiction models the porous concrete aggregates as hardcore materials, the cementitious materials as a soft shell, and the voids as the bulk phase. The soft shell encases the hardcore particles and is situated inside the bulk phase. Figure 7 illustrates four distinct porosities: (i) 27.3%, (ii) 22.4%, (iii) 18.0%, and (iv) 14.1%. Aggregates are shown as dark circles, cementitious elements are represented in white, and voids are indicated in black [143].

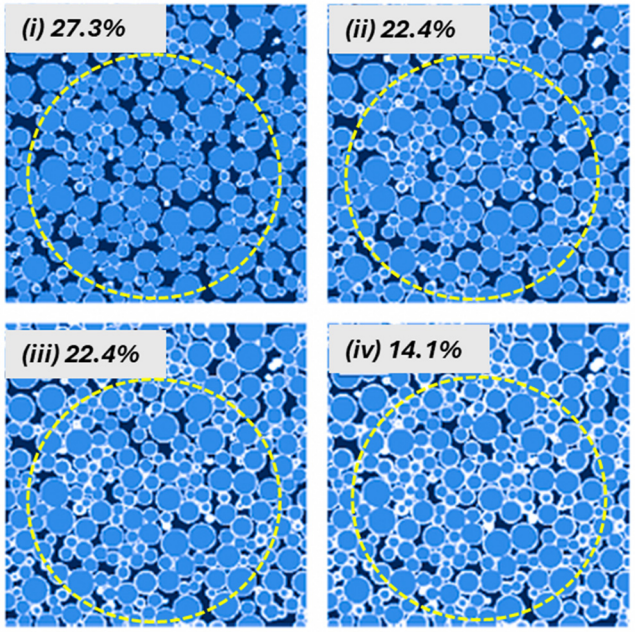


Figure 7. Two-dimensional images from three-dimensional virtual porous concrete microstructures based on a hybrid HCSS model [143].

A different virtual microstructure of porous concrete was also compared with the HCSS model. This technique relies on filtered correlation reconstruction models that emphasise percolation and transportation instead of the aggregate structures shown in the HCSS model. This method depicts porosities as black regions, whilst aggregates and cementitious substances are shown as white regions. This approach is essential for forecasting porosity [143,144].

4.5. Image Analysis Method

Other researchers used the image analysis method to find porous concrete properties, such as average porosity and pore size distribution [47,145,146]. This method provides a much better resolution of the porosity distribution than the Haselbach and Freeman [147] method while avoiding some of the measurement technique drawbacks encountered by [148]. While this method can measure the porosity distribution in any direction, this paper focuses on vertical porosity distribution because of its importance to the hydraulic behaviour in porous pavements. Researchers have extensively used image analysis techniques to ascertain critical characteristics of porous concrete, such as average porosity and pore size distribution [32,149,150]. This methodology provides markedly enhanced resolution of porosity distribution relative to the method suggested by Haselbach and Freeman [147] while also mitigating some measurement limits faced by De Somer and De Winne [151]. This method's primary benefit is its capacity to quantify porosity distribution in all directions, offering a thorough evaluation of the internal structure of porous concrete. This research especially examines vertical porosity distribution owing to its significant impact on the hydraulic performance of porous pavements, notably regarding water infiltration and drainage efficiency [152].

Multiple techniques were employed to evaluate porosity. The image analysis method involves slicing a cylindrical specimen (100 mm in diameter and 150 mm in length) into 50 mm thick sections, yielding 6 to 18 surfaces. These surfaces are polished and painted white, and then scanned onto a transparent plastic sheet in greyscale using a flatbed scanner at a resolution of 300 dpi. Images without edge effects are further processed using image analysis software (ImageJ, National Institutes of Health, USA). The greyscale scans are cropped into circular images of 570 pixels (corresponding to 95 mm in diameter), from which 400 × 400-pixel square segments are extracted to analyse pore structure characteristics. The area of each pore is measured, summed, and divided by the total image area to determine the pore area fraction [47]. This approach is confined to laboratory applications because of its need for specialised equipment, controlled environments, and sample preparation. It is presently inapplicable for in situ or field-based assessments of pore structure. Recently, Abousnina [153] used image analysis with a different software TBitmap (as shown in Figures 8 and 9). Several images were taken under a microscope set at a magnification of 65 times and analysed using image analysis that involved resin colour analysis to identify the pixels in the image as pores. Microscopy was conducted 28 days after the compression test.

High-resolution images were used to determine the number of samples required to accurately characterise porosity, due to their ability to detect smaller pore sizes [154]. Since a higher resolution covers a smaller surface area, more images are needed to provide a reliable porosity estimate. The minimum number of representative image samples was established based on the physical properties of the specimens. Porosity was measured by randomly selecting a subset of images corresponding to the specimen's surface area. Each image was taken at the highest magnification of the optical microscope, covering only 0.09 cm^2 of the total surface. Therefore, at least ten images—representing approximately 20% of the specimen's total surface area—were collected as recommended. These ten

images were used for all subsequent porosity analyses. As shown in Figure 10, the standard deviation remained relatively stable when ten or more images were used.

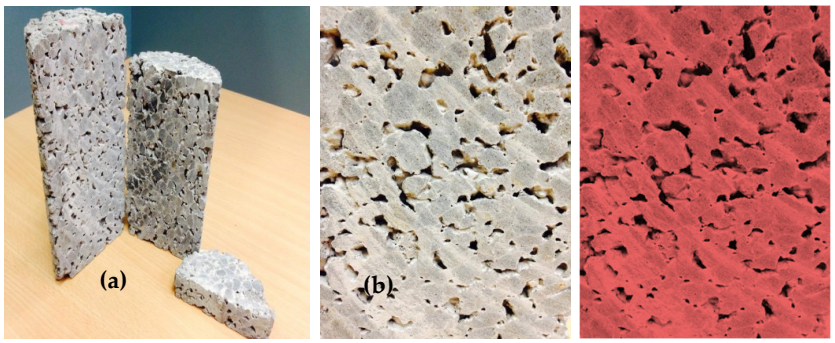


Figure 8. Example image of specimens' surface showing pores ((**a**) natural colour of the surface, and (**b**) after readjusting the colour to be readable by the software).

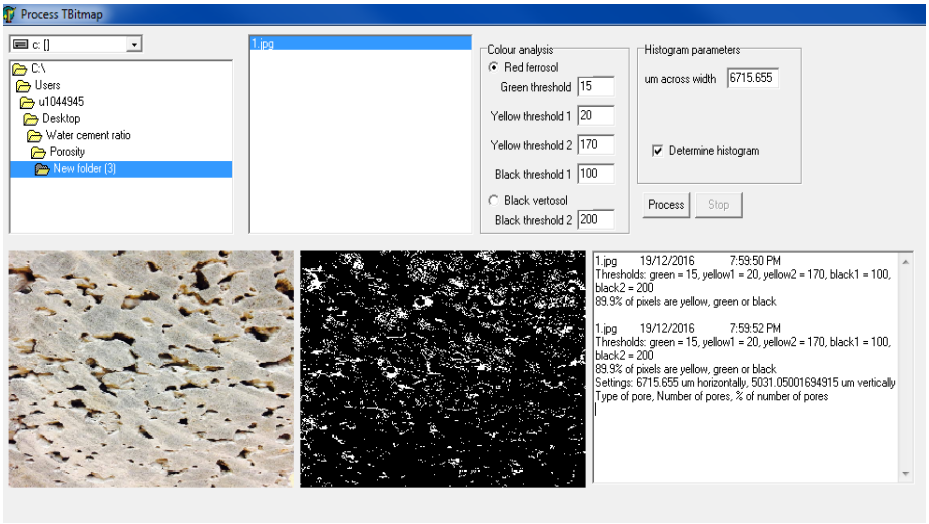


Figure 9. Example analysis screen using TBitmap software for a surface image.

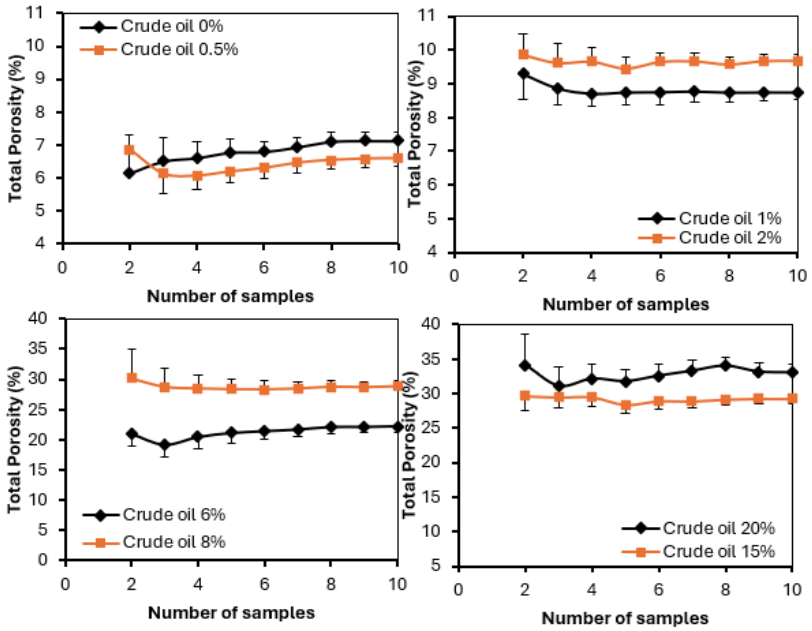


Figure 10. Standard deviation of samples of mortar images [154].

4.6. Image Analysis vs. Mathematical Model

Image analysis was utilised to scan samples and generate a volumetric representation [155]. The results were presented in terms of a void continuity index (VCI), which indicates whether pore spaces lead to radial (horizontal) or end (vertical) exits, as well as the direction of successful continuity propagation from the central cross-section [155,156]. The study found a linear relationship between compressive strength and void ratio, as illustrated in Figure 11. According to this correlation, a lower void content corresponds to higher compressive strength. Additionally, a relationship between compressive strength and void content was established, as shown in Equation (25).

$$\text{Compressive strength (MPa)} = 4762.1 - 97.16 \times [\text{void ratio (\%)}] \quad (25)$$

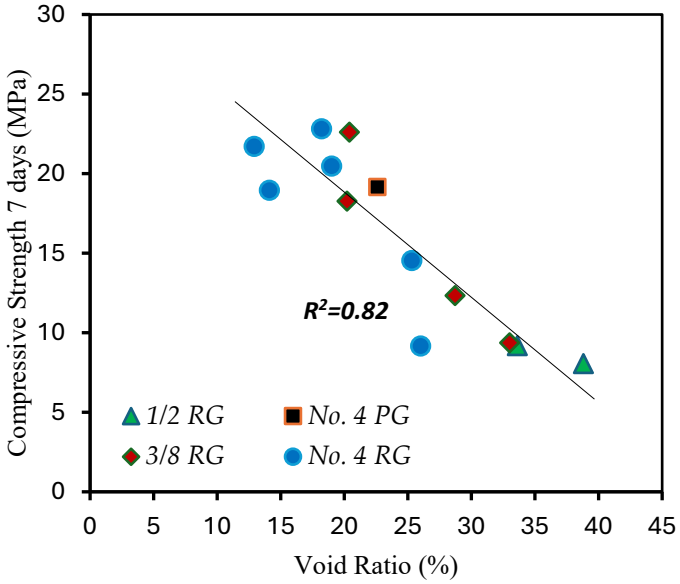


Figure 11. Relationship between compressive strength and void content [157].

On the other hand, Matsuo, et al. [142] performed a compressive strength test developed by the Japan Concrete Institution. Figure 11 shows the relationship between compressive strength and total void ratio. A linear relationship can be seen, and the compressive strength decreases from 20 MPa to 10 MPa when the total porosity content was increased from 20% to 30%.

Similarly, Zhong and Wille [77] investigated the effect of total porosity on the compressive strength of porous concrete. They found that a reduction in total porosity, combined with enhanced matrix strength, led to increased compressive strength. In the present study, porosity was determined by measuring the weight difference between oven-dried and water-saturated specimens. A similar method was used by [158], where the total porosity was determined using a three-by-six-inch cylinder sample by taking the weight difference between an oven-dried sample and an underwater sample [159]. As shown in Figure 12, the reduction in strength as a function of the void ratio is linear.

On the other hand, a study conducted by Maguesvari and Narasimha [160] investigated the characterisation of porous concrete for pavement applications. In their study, the total porosity was determined by an angularity number method as per IS: 2386-part-1. Although the total porosity increased as the strength decreased, they concluded that there is a definite correlation between total void and compressive strength; the relationship between the strength and total porosity was not linear compared to the previous studies mentioned earlier (Figure 13).

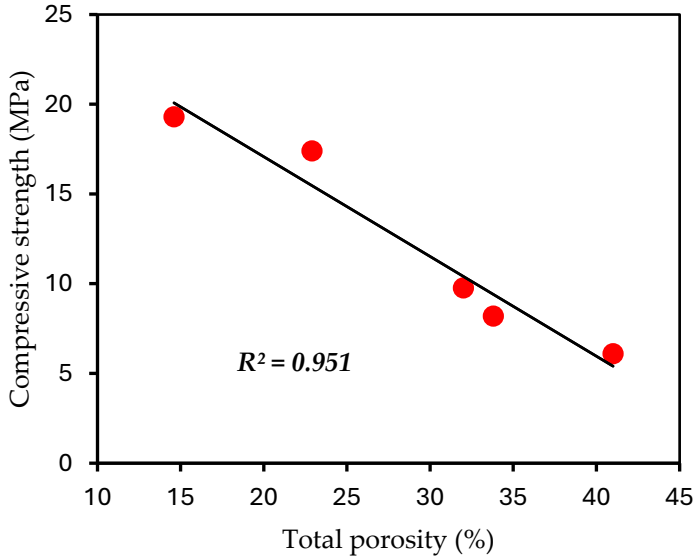


Figure 12. Relationship between compressive strength and void content [77].

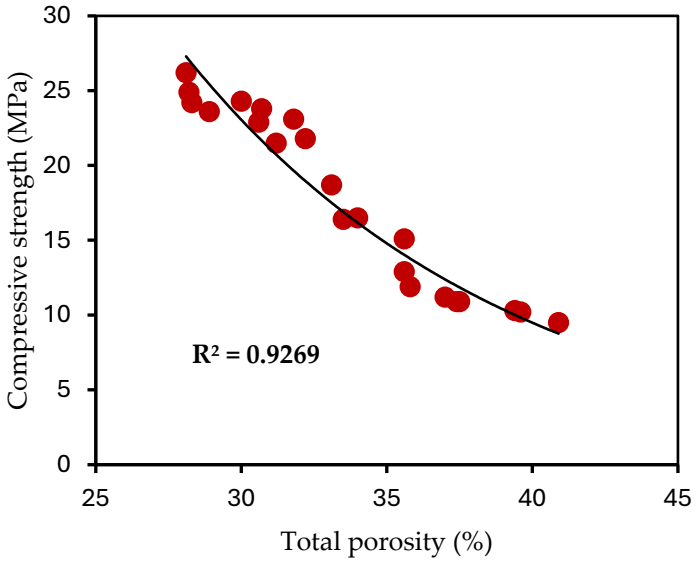


Figure 13. Relationship between compressive strength and void content [160].

Similar results were obtained in [161] when the authors used a mathematical model to estimate the total porosity and compared it with the compressive strength of porous concrete. An exponential regression equation can be fitted to the data from their study. The fitted exponential curve yields the following equation: r = 231 exp (0.09p), with an R^2 value of 0.90. A similar model was presented in [162] and the only difference was the value of R^2 (0.96), which is higher than the value of 0.90 obtained by Lian, et al. [161].

5. Discussion

5.1. Comparison of Properties of Porous Concrete and Conventional Concrete

The characteristics of porous concrete were examined and contrasted with those of standard concrete, as seen in Table 3. A significant challenge in applying porous concrete is the variability in workability between laboratory-developed mixes and those produced in the field. It is important to accurately assess porous concrete's workability and verify that the formulated concrete mixes are appropriate for specific compaction techniques and site circumstances. Porous concrete often exhibits a lower slump than traditional concrete; hence, researchers have used several admixtures to enhance workability without signifi-

cantly increasing water content. Numerous studies have used water-reducing admixtures to enhance workability [32,41,74]. The placement and compaction of the concrete vary significantly from regular concrete due to the earthy material's very poor workability. The average density of standard concrete is 2400 kg/m^3, while that of porous concrete ranges from 1600 to 2000 kg/m^3. Consequently, the porous concrete exhibited a reduced density of around 25% compared to traditional concrete. The age of the concrete did not affect the density of porous and conventional concrete [34,163–166].

Porous concrete demonstrated inferior strength relative to normal concrete. The average compressive strength of conventional concrete was around 46 MPa, but the compressive strength of porous concrete varied from 2.5 MPa to 34.5 MPa [167–169]. Porous concrete is anticipated to have less compressive strength owing to its increased porosity relative to traditional concrete. Concrete is well recognised to increase in strength over time. Nonetheless, the strength of porous concrete exhibited only a marginal enhancement over time in comparison to ordinary concrete. This tendency is due to cement hydration, which is essential for the strength development of conventional concrete but has somewhat less impact on the characteristics of porous concrete. The water permeability of porous concrete is much greater than that of standard concrete. The water permeability of porous concrete is around 0.34 cm/s, while ordinary concrete has a permeability of about 2.39×10^{-11} m/s [170]. The coefficient of variance varies between 7.3% and 42%. The water permeability of porous concrete is greatly determined by pore structure, which is impacted by compaction and grading. The elastic modulus of porous concrete ranges from 8 to 15 GPa (25% to 18% porosity), while ordinary concrete has a modulus of 30 GPa [171,172].

Table 3. A comparison of the properties of porous concrete and conventional concrete.

Properties	Porous Concrete	Conventional Concrete	References
Workability	80 mm	70 mm	[162]
Compaction factor	0.82	0.85	
Density	1500 to 2200 Kg/m^3	2400 Kg/m^3	[162–164]
Compressive strength 28 days	2.5–34.5 MPa	46.5 MPa	[119,172–174]
Permeability	0.34 cm/s, or 200 L/m^2/min)	2.39×10^{-11} m/s	[79,162,173,175]
Elastic modulus	8–15 GPa (25–18% porosity).	30 GPa	[117,140,172]
Porosity	15% to 30%	1–3%	[63,85,176]

The porosities of conventional and porous concrete with various combinations of binder ingredients were compared [177]. Porous concrete has much more porosity than traditional concrete throughout various curing durations. The average porosity of porous concrete is 0.34, whereas the porosity of ordinary concrete is 0.08 [178]. The porosity of ordinary concrete diminishes with age, attributed to the ongoing hydration of the cement. The porosity of the porous concrete remained unaffected by the concrete's age. The various pore structures were accountable for this behaviour. Its age influences the porosities of typical concrete. The porosity in porous concrete mostly results from enormous air spaces, which exceed the size of the pores in cement paste. The porosity of porous concrete is affected by aggregate grading and compaction. Consequently, the porosity of porous concrete is largely unaffected by the ageing process of the material.

5.2. Influence of the Factors on the Properties

Porous concrete has gained global popularity as an efficient stormwater runoff control solution. Numerous investigations have been undertaken by researchers to enhance traditional porous concrete pavement [179,180]. The primary issue with porous concrete is its strength, which is compromised by its elevated void content, making it challenging to achieve high strength. The strength of porous concrete is determined by its overall

porosity, which is influenced by several parameters, including binder types, aggregate type, aggregate grading, mix composition, and compaction. Various sorts of additives have been investigated to enhance the cement binder. Despite extensive research on basic facts, the ideal conditions for producing high-quality porous concrete remain undetermined. The collective physical attributes, including size, shape, and distribution, significantly influence the mechanical, durability, and permeability properties of porous concrete pavements [181,182]. The results suggest that the aggregate properties in porous concrete must be regulated due to the thin cement paste, which facilitates water infiltration into the pores of individual aggregates, consequently increasing the likelihood of freeze–thaw damage and durability cracking in these pavements [183]. Regarding mix design criteria and testing methodologies, there is no standardised mix design approach for porous concrete, resulting in non-comparable outcomes across various research studies. The testing procedures designated for standard concrete are being used for porous concrete, which has prompted many concerns among researchers owing to variations in material compositions.

5.3. Effect of Porosity Measurement Methods

The porosity of porous concrete is an important variable needed for pavement system design and material comparisons. As mentioned earlier, many researchers have investigated the porosity of porous concrete. However, the exact details of the methodology for its determination have not been clearly shown [80].

Some studies have reported on the characteristics of porous concrete but have not clearly specified the testing methodologies used to determine porosity [184]. Other researchers have investigated the water purification properties of porous concrete and estimated porosity using the water displacement method, referring to it as the void ratio without citing any standardised procedure [185,186]. ASTM International has established protocols for evaluating porosity-related properties in concrete materials. ASTM C29/C29M-97 outlines the standard procedure for measuring bulk density and void content in loose aggregates, which are typically unshaped and susceptible to compaction. Additionally, ASTM C127 and ASTM C128 provide standard methods for determining the specific gravity and absorption of coarse and fine aggregates, respectively. However, none of these procedures are specifically designed for application to porous concrete. Research conducted by Belgian scholars identified a depth-dependent porosity distribution in pavement systems combining conventional and porous concrete. In that study, differential porosity was measured using a water displacement technique, where the specimen was incrementally submerged, and its submerged mass was recorded at each stage [151]. While this method yielded valuable insights into porosity variation with depth, it is not intended for field-based material testing.

The literature highlights that the InstroTek Corelok System employed a distinctive approach, using vacuum technology to enhance air removal and promote water infiltration into the porous matrix. Although innovative, this system is now considered obsolete and has been superseded by a revised version of the AASHTO Standard Method of Test for Bulk Specific Gravity of Compacted Bituminous Mixtures Using Saturated Surface-Dry Specimens (T 166), which typically results in values 2–4% higher [187]. However, this method is not suitable for porous concrete without modification, as typical specimens can absorb well over 2% of their solid mass in water. Moreover, the large, interconnected voids in porous concrete allow water to drain too rapidly upon removal from the water tank, making it difficult to accurately determine the saturated surface-dry mass without procedural adjustments. Previous research has explored alternative methods to assess porosity distribution. One of the earliest efforts by De Somer and De Winne [151] involved suspending a porous specimen in a container while incrementally adding known volumes

of water. By tracking the corresponding rise in water level, porosity was calculated at various heights along the specimen. Despite its usefulness, this method presented several limitations. Capillary action caused excessive water absorption, leading to overestimated porosity in some areas. Additionally, the gradual immersion process allowed for air entrapment in certain pores—air that might escape using other testing methods—potentially resulting in underestimated porosity values. This issue becomes more pronounced in specimens with lower porosity.

A new test method for porosity measurements of porous concrete was presented by Montes, et al. [80]. They applied the Archimedes principle and used standard materials and laboratory equipment. Discrepancies among different operators at various testing facilities have been reported, with variations in porosity measurements of approximately 2.2%. In addition, several alternative methods exist for characterising permeable voids. One approach involves statistical analysis of pore size distribution using micrographs and manual counting, while another measures the rate of water absorption over time, as described in Sections 4.2 and 4.3. However, these methods are often time-consuming and may require specialised equipment, making them unsuitable for routine quality control applications [80,188,189]. More recently, an image-analysis-based method has been applied to evaluate porosity distribution in porous pavement samples [47,145,157]. This technique provides significantly higher resolution than previous methods [147] and addresses several of the measurement limitations encountered in earlier studies [151]. Additionally, it enables porosity distribution to be assessed in any spatial orientation [150]. This method can measure the porosity distribution in any direction [148].

It is concluded that the result in porosity measurements agrees with the existing porosity test, and there is no statistically significant difference between the image analysis measurements and the vacuum porosity method when calculating the average porosity and general agreement by all the methods for porosity distribution. This shows that image analysis can be considered a practical tool to be used to estimate the total porosity; however, further comparison is required between this method and the method used by Abousnina, et al. [190] (imaged analysis with a different software TBitmap). This method gives more details of the pore size percentages (%) as explained earlier, which will provide more information about the total percentage for each size. Thus, further investigation can be carried out to overcome the issue of clogging by trying to reduce the size of the total porosity that causes clogging. Clogging is perceived as a major problem for any type of permeable pavement, and hence, using a proper method of estimating the porosity with more details, such as the percentage of each size, will help to understand the pore structure, which will help to solve other issues such as clogging.

The porosity of porous concrete is a critical parameter for pavement system design and material evaluations. Numerous scholars have already examined the porosity of porous concrete. Nevertheless, the specifics of the process for its conclusion have not been explicitly presented [191]. Some have documented the characteristics of certain porous concretes but have not detailed the precise testing methodology used to determine the porosities [183]. Other researchers have used specific water purification characteristics of porous concrete and assessed porosity by the water displacement technique, although they have termed it a void ratio without citing a standard procedure [149,192]. ASTM International has established testing protocols for assessing porosity in concrete materials. ASTM C 29/C 29M-97 is the standard for evaluating bulk density and voids in loose aggregates. This test is used for aggregates that lack a definite shape and are prone to compaction. The ASTM Standard Test Method for Specific Gravity and Absorption of Coarse Aggregate (C 127) and the ASTM Standard Test Method for Specific Gravity and Absorption of Fine Aggregate (C 128–97) are standards utilised to assess the specific gravity and absorption of coarse and

fine aggregates. Nevertheless, none of these techniques are tailored for use with porous concrete. Research conducted by Belgian scholars identified a porosity–depth distribution in porous pavements composed of regular cement concrete and porous concrete. The technique used to ascertain the differential porosity distribution with depth included a water displacement approach, whereby the porous concrete specimen was gradually immersed in water, and the submerged mass was documented at intervals throughout the submersion process [193,194]. This approach provided significant insights into the porosity variance in concrete samples; nevertheless, it is not designed for field material testing. The InstroTek CoreLok system, previously prevalent for assessing the bulk specific gravity of absorptive asphalt mixtures, is now deemed less appropriate due to revisions in standardised testing protocols. The AASHTO T 166 method has been updated to suggest alternative procedures, including AASHTO T 275 or T 331, for specimens exhibiting high absorption or interconnected voids [135]. In porous concrete, the interconnected pore structure frequently permits water to constitute over 2% of the specimen's solid mass, surpassing the absorption limit specified in T 166. Moreover, upon removal of the specimen from the water tank, water swiftly drains from the large pores, complicating the precise identification of the saturated surface-dry (SSD) condition. Precise measurement of SSD mass is essential for ascertaining bulk specific gravity, and without procedural adjustments—such as regulated timing or surface drying methods—this condition cannot be reliably attained. Consequently, T 166 is inappropriate for porous concrete unless specific modifications are made to address its elevated porosity and swift drainage properties.

A novel testing method for measuring the porosity of porous concrete was introduced using the Archimedes principle and standard laboratory equipment [195]. To enhance accuracy in porosity assessment, a new approach was developed, resulting in a discrepancy of approximately 2.2% porosity among operators at different testing sites [196]. To improve measurement consistency, a new method was introduced, alongside other techniques for delineating permeable areas. One approach involves statistical analysis of pore size distribution using micrographs and statistical counts, while another measures the temporal water adsorption rate, as detailed in Sections 4.2 and 4.3. However, these methods can be time-consuming and may require specialised equipment, making them impractical for quality control assessments. Montes et al. developed this method to enhance efficiency and reliability in porosity measurement [197,198].

A novel technique for assessing the porosity distribution of a porous pavement sample by image analysis has been used recently [199–201]. This approach offers significantly improved resolution of porosity distribution compared to prior techniques while circumventing some measurement methodology limitations faced by earlier investigations [202,203]. This approach can measure porosity dispersion in any direction. The findings indicate that the porosity measurements align with the established porosity test, revealing no statistically significant difference between the image analysis measurements and the vacuum porosity method in calculating average porosity, as well as overall consistency across all methods concerning porosity distribution. This indicates that image analysis may be regarded as a realistic technique for estimating total porosity; nevertheless, more comparisons are necessary between this approach and that used by Abousnina [154], (image analysis using the alternative program TBitmap). This approach elucidates the percentages of pore sizes, as previously described, so offering further insights into the overall proportion for each size. Consequently, more research may be conducted to address the clogging problem by attempting to decrease the overall porosity that contributes to it. Clogging is regarded as a significant concern for all forms of permeable pavement; thus, using an accurate approach to estimate porosity, including the proportion of each particle size, would enhance the understanding of pore structure and assist in addressing related problems such as clogging.

5.4. Optimal Pore Characteristics in Porous Concrete

The porosity of ordinary porous concrete may vary anywhere from 15 to 25 percent, with the National Ready Mix Concrete Association requiring a minimum porosity of 15 percent [74,114]. Interconnected pores, capillary pores, and dead-end pores are the three types of pores that may be used to classify the total porosity of the porous concrete mixture. Therefore, it is predicted that the total porosity will have a substantial effect on the hydraulic conductivity; however, matrix workability and aggregate size also have an impact on this parameter. As a consequence of this, it is of the utmost importance to locate and define a particularly accurate method for determining total porosity.

5.5. Development of Standard Specifications

Over more than twenty years, porous concrete has shown satisfactory performance in the field; yet, when it comes to standardised testing, porous concrete typically demonstrates poor performance [204]. Some approaches have been tried out since porous concrete does not have any standardised testing procedures for many characteristics. Some of these methods, such as the link between the strength and the porosity and the influence of the calculation method used for the total porosity, have been addressed in this work. The fact that this is the case shows that the various ways of calculation that are used to comprehend the connection between porosity and strength may not be able to accurately explain the effectiveness of the various approaches that are utilised in estimating the total porosity. Because of this, there is a need for more research into the various techniques that are used in the estimation of the total porosity and the impact that it has on the characteristics of porous concrete. Various approaches to determining the porosity of porous concrete led to a variety of relationships between the porosity and the strength of the material. This was due to the extensive interconnected void system that is present in porous concrete. The establishment of global standard procedures for porous concrete is essential, as it would not only enhance the understanding of its material behaviour but also facilitate its widespread implementation across diverse geographic regions.

5.6. Proposed Guidelines for Overcoming the Challenges of Porous Concrete

Porous concrete provides numerous benefits, particularly its capacity to diminish stormwater runoff—a key functional aim of its design [205,206]. As was noted previously, there are many advantages to utilising porous concrete. Porous concrete can also reduce the amount of noise that is produced by cars that are driving on concrete pavements. This is because it reduces the noise of the contact between the tyre and the pavement. The sound is absorbed by porosity in the pavement [54,207]. Furthermore, it can filter contaminants present in stormwater runoff that would otherwise infiltrate the ground. As a result of its ability to absorb runoff water, porous concrete helps to preserve this natural resource [37].

On the other hand, using porous concrete presents several obstacles, the most significant of which are the absence of standard criteria and integrity between the product components. Compared to ordinary concrete, permeable concrete can create a more significant number of voids inside the structure, resulting in increased rates of water penetration and high air exchange. One of the major obstacles preventing the development of permeable pavements is the perception that these pavements do not possess sufficient structural strength. The necessity for increased porosity for therapeutic reasons is the primary factor that has led to this situation. Options such as the following are available for resolving this issue:

- By employing fibre-reinforced porous concrete, it has been shown that the porous concrete displayed much better rates of permeability than the control mix. This was demonstrated by the fact that the Ultra-Fibre was used. There was a 234% increase in

permeability with the addition of Ultra-Fibre at a dose rate of 1.779 kg/m^3. All dose rates increased in split tensile strength, with the highest increase occurring at a dosage rate of 0.889915 kg/m^3, which was 24%. Consequently, this suggests that the use of fibre may be able to assist in overcoming the lack of integrity between the components, which will increase the strength. In addition, recent research that was carried out by Abousnina [154] showed that the compressive strength was improved when a fine aggregate that was contaminated with light crude oil was used. After careful consideration, it has been determined that the compressive strength of light crude oil, which was 1% of the total, was 18% greater than that of the samples that were not polluted. In their study on the effect of crude oil contamination on the compressive strength of concrete, Osuji and Nwankwo [208] concluded that the presence of crude oil in the production of concrete hinders the formation of bonds between the constituent materials and causes segregation. This finding has been supported by their findings.

- The impact of light crude oil on permeability was examined, revealing a considerable increase in permeability with up to 6% crude oil contamination. This was executed because the sand was already covered with crude oil, enhancing its hydrophobicity and expediting water movement [209]. This indicates that light crude oil might serve as an addition to enhance the strength and permeability of porous concrete more effectively.
- The development of standard processes for structural design involves a mixed design and demonstrates the correct measurement technique. This is because, as was shown previously, there is a lack of consensus on the link between strength and porosity. Nevertheless, it has been shown that the use of image analysis to measure the porosity distribution of porous concrete yields porosity readings that are in good agreement with the practices that are currently utilised for porosity testing. Since it may be used to evaluate porosity in any direction, this approach offers a much higher resolution of the porosity distribution [210]. In addition to this, it has been shown that there is no statistically significant difference between the data obtained by image analysis and the vacuum porosity technique when it comes to calculating the average porosity and that there is general agreement among all of the approaches about the porosity distribution [211]. In addition, the vertical porosity distribution that was evaluated by employing the image analysis approach was in good agreement with the empirical models [212]. This approach enhances the understanding of porosity by providing detailed insights into the pore structure and identifying primary pores that may contribute to clogging [153,213]. A comparison between the previously described image analysis method and one developed using TBitmap software was conducted, with the latter offering improved resolution and more comprehensive porosity data.

6. Conclusions

This paper analysed current research on the mechanical properties of porous concrete compared to regular concrete. The main goal was to emphasise the relevance of porous concrete, identify its major issues, and provide potential remedies. The significant findings of this study are as follows:

- Previous studies have shown that porous concrete has lower compressive strength, density, and elastic modulus while increasing permeability due to its higher porosity when compared to regular concrete.
- Several factors influence the performance of porous concrete; nevertheless, porosity and binder type are critical in achieving the best results. The strength of porous concrete is primarily dictated by total porosity, which is regulated by factors such as binder type, aggregate type, aggregate grading, mix composition, and compaction.

- Researchers studied numerous approaches for estimating the porosity of porous concrete, which resulted in inconsistencies in the recorded relationship between porosity and strength. Image analysis has shown the best accuracy among these methods, providing high-resolution data on porosity distribution and allowing measurements in various orientations.
- There is a continuing debate about whether effective or total porosity has a more significant impact on the properties of porous concrete. Recent research shows that effective porosity alone cannot predict hydraulic conductivity, but compressive strength is more closely linked with total porosity. As a result, overall porosity must be considered the primary criterion in evaluating the performance of porous concrete.
- A standardised porosity measurement procedure must be adopted to accurately establish the relationship between porosity and compressive strength. Developing universal structural design guidelines and consistent porosity assessment methods will enhance the understanding of porous concrete behaviour and ensure reliability and uniformity in strength evaluation.

By addressing these challenges and improving measurement methods, porous concrete may be utilised as a sustainable construction material with exceptional mechanical performance.

Author Contributions: Conceptualisation, R.A. and B.B.; methodology, R.A. and B.B.; formal analysis, R.A., B.B., M.H.A. and V.V.; investigation, R.A., F.A., B.B., M.H.A. and V.V.; data curation, R.A. and B.B.; writing—original draft preparation, R.A. and B.B.; writing—review and editing, R.A., M.H.A. and V.V.; funding acquisition, F.A. All authors have read and agreed to the published version of the manuscript.

Funding: The research was funded by Prince Sattam bin Abdulaziz University through project number PSAU/2024/01/99513.

Data Availability Statement: The data is contained within the article.

Conflicts of Interest: The authors declare no conflicts of interest.

References

1. Xie, N.; Akin, M.; Shi, X. Permeable concrete pavements: A review of environmental benefits and durability. *J. Clean. Prod.* **2019**, *210*, 1605–1621. [CrossRef]
2. Elizondo-Martínez, E.-J.; Andres-Valeri, V.-C.; Jato-Espino, D.; Rodriguez-Hernandez, J. Review of porous concrete as multifunctional and sustainable pavement. *J. Build. Eng.* **2020**, *27*, 100967. [CrossRef]
3. Moretti, L.; Di Mascio, P.; Fusco, C. Porous concrete for pedestrian pavements. *Water* **2019**, *11*, 2105. [CrossRef]
4. Sánchez-Mendieta, C.; Galán-Díaz, J.J.; Martinez-Lage, I. Relationships between density, porosity, compressive strength and permeability in porous concretes: Optimization of properties through control of the water-cement ratio and aggregate type. *J. Build. Eng.* **2024**, *97*, 110858. [CrossRef]
5. Uma Maguesvari, M. Studies on Pervious Cement Concrete and Fly Ash-Cement Concrete as a Pavement Material. Ph.D. Thesis, Department of Civil Engineering, PEC, Pondicherry University, Puducherry, India, 2017.
6. Tie, T.S.; Mo, K.H.; Putra, A.; Loo, S.C.; Alengaram, U.J.; Ling, T.-C. Sound absorption performance of modified concrete: A review. *J. Build. Eng.* **2020**, *30*, 101219. [CrossRef]
7. Fediuk, R.; Amran, M.; Vatin, N.; Vasilev, Y.; Lesovik, V.; Ozbakkaloglu, T. Acoustic properties of innovative concretes: A review. *Materials* **2021**, *14*, 398. [CrossRef]
8. Jaya, R.P. Porous concrete pavement containing nanosilica from black rice husk ash. In *New Materials in Civil Engineering*; Elsevier: Amsterdam, The Netherlands, 2020; pp. 493–527.
9. Carpio, M.; González, Á.; González, M.; Verichev, K. Influence of pavements on the urban heat island phenomenon: A scientific evolution analysis. *Energy Build.* **2020**, *226*, 110379. [CrossRef]
10. Bateni, N. Permeable Road Pavement with Subsurface Precast Micro-Detention Storage: A Green Pavement Practice. Ph.D. Thesis, University of Malaya, Kuala Lumpur, Malaysia, 2020.

11. Muthusamy, K.; Rasid, M.H.; Jokhio, G.A.; Budiea, A.M.A.; Hussin, M.W.; Mirza, J. Coal bottom ash as sand replacement in concrete: A review. *Constr. Build. Mater.* **2020**, *236*, 117507. [CrossRef]
12. Yun, C.M.; Rahman, M.R.; Kuok, K.K.; Sze, A.C.P.; Seng, A.L.K.; Bakri, M.K.B. Pervious Concrete Properties and Its Applications. In *Waste Materials in Advanced Sustainable Concrete: Reuse, Recovery and Recycle*; Springer: Berlin/Heidelberg, Germany, 2022; pp. 1–23.
13. Paul, S.C.; Van Rooyen, A.S.; van Zijl, G.P.; Petrik, L.F. Properties of cement-based composites using nanoparticles: A comprehensive review. *Constr. Build. Mater.* **2018**, *189*, 1019–1034. [CrossRef]
14. Xiao, J.; Lv, Z.; Duan, Z.; Zhang, C. Pore structure characteristics, modulation and its effect on concrete properties: A review. *Constr. Build. Mater.* **2023**, *397*, 132430. [CrossRef]
15. Salih, N.M.; Al-Majmaie, S.M.; Muhammad, Z.A. The porous–permeable zones in heterogeneous carbonate reservoirs: A case study from Amara Oilfield, Iraq. In Proceedings of the 4th International Electronic Conference on Geosciences, Online, 1–15 December 2023; p. 35.
16. Adebayo, I.H. Engineering Properties of Pervious Concrete Containing Palm Oil Clinker Aggregate. Ph.D. Thesis, University of Malaya, Kuala Lumpur, Malaysia, 2018.
17. Revilla-Cuesta, V.; Faleschini, F.; Zanini, M.A.; Skaf, M.; Ortega-López, V. Porosity-based models for estimating the mechanical properties of self-compacting concrete with coarse and fine recycled concrete aggregate. *J. Build. Eng.* **2021**, *44*, 103425. [CrossRef]
18. Malozyomov, B.V.; Martyushev, N.V.; Kukartsev, V.V.; Tynchenko, V.S.; Bukhtoyarov, V.V.; Wu, X.; Tyncheko, Y.A.; Kukartsev, V.A. Overview of methods for enhanced oil recovery from conventional and unconventional reservoirs. *Energies* **2023**, *16*, 4907. [CrossRef]
19. McAneny, G.T. Sensitivity of Shear and Longitudinal Velocity to Compression and Shear Stress Paths in Cohesive Soils. Master's Thesis, Tufts University, Somerville, MA, USA, 2022.
20. Zhao, H.; Geng, Q.; Liu, X. Influence of freeze–thaw cycles on mechanical properties of pervious concrete: From experimental studies to discrete element simulations. *Constr. Build. Mater.* **2023**, *409*, 133988. [CrossRef]
21. Chen, S.; Wang, Y.; Dai, W.; Yang, H.; Wang, D.; Lv, Y. Recycled aggregate porous concrete: Pore structure, clogging properties and models. *Constr. Build. Mater.* **2024**, *417*, 135344. [CrossRef]
22. Wei, Y.; Chen, X.; Chai, J.; Qin, Y. Correlation between mechanical properties and pore structure deterioration of recycled concrete under sulfate freeze-thaw cycles: An experimental study. *Constr. Build. Mater.* **2024**, *412*, 134794. [CrossRef]
23. Prasittisopin, L.; Tuvayanond, W.; Kang, T.H.-K.; Kaewunruen, S. Concrete Mix Design of Recycled Concrete Aggregate (RCA): Analysis of Review Papers, Characteristics, Research Trends, and Underexplored Topics. *Resources* **2025**, *14*, 21. [CrossRef]
24. Brammer, R. Exploring Lean-Agile Adoption in Publishing: MVBs, Porous Books and Feedback Loops. Ph.D. Thesis, University of Westminster, London, UK, 2024.
25. Giao, P.H.; Nguyen, P.H. Porosity. In *Encyclopedia of Mathematical Geosciences*; Springer: Berlin/Heidelberg, Germany, 2023; pp. 1086–1090.
26. Dey, S.; Kumar, V.P.; Goud, K.; Basha, S. State of art review on self compacting concrete using mineral admixtures. *J. Build. Pathol. Rehabil.* **2021**, *6*, 18. [CrossRef]
27. Katkar, B.S.; Gupta, D.N. Utilization Of Building Demolished Waste Aggregates In Pervious Concrete. *Int. J. Adv. Res. Sci. Eng.* **2017**, *6*, 1009–1023.
28. da Costa, F.B.P.; Haselbach, L.M.; da Silva Filho, L.C.P. Pervious concrete for desired porosity: Influence of w/c ratio and a rheology-modifying admixture. *Constr. Build. Mater.* **2021**, *268*, 121084. [CrossRef]
29. Figueroa, N.N.; Brante, A.; Leclerc, J.-C.; Salgado, P.; Oyarzo-Vera, C. The physical and mechanical consequences of incorporating industrial residues into mortar and concrete mixtures for eco-friendly marine constructions. *Innov. Infrastruct. Solut.* **2024**, *9*, 466. [CrossRef]
30. Kevern, J.T.; Schaefer, V.R.; Wang, K. Evaluation of pervious concrete workability using gyratory compaction. *J. Mater. Civ. Eng.* **2009**, *21*, 764–770. [CrossRef]
31. Hu, J.; Ma, T.; Zhu, Y.; Huang, X.; Xu, J. A feasibility study exploring limestone in porous asphalt concrete: Performance evaluation and superpave compaction characteristics. *Constr. Build. Mater.* **2021**, *279*, 122457. [CrossRef]
32. Li, Q.; Zheng, J.; Fu, M. Experimental investigation on influence of molding methods on properties of pervious concrete. In Proceedings of the Journal of Physics: Conference Series; IOP Publishing: Bristol, UK, 2022; Volume 2148, p. 012055.
33. Akkaya, A.; Çağatay, İ.H. Investigation of the density, porosity, and permeability properties of pervious concrete with different methods. *Constr. Build. Mater.* **2021**, *294*, 123539. [CrossRef]
34. Venkati, B.; Vanik, M. Applications and development of pervious concrete in pavement. *J. Resour. Manag. Technol* **2021**, *12*, 331–338.
35. Wong, W.Y. Strength Properties of Lightweight Foamed Concrete with 30 kg/m^3 Steel Fiber. Ph.D. Thesis, UTAR: Kampar, Perak, Malaysia, 2023.

36. Othman, R.; Jaya, R.P.; Muthusamy, K.; Sulaiman, M.; Duraisamy, Y.; Abdullah, M.M.A.B.; Przybył, A.; Sochacki, W.; Skrzypczak, T.; Vizureanu, P. Relation between density and compressive strength of foamed concrete. *Materials* **2021**, *14*, 2967. [CrossRef]
37. LO. Marchioni, M.L. Porous Surfaces for Permeable Pavement: Clogging and Filtration Mechanisms. Ph.D. Thesis, Politecnico di Milano, Milan, Italy, 2018. Available online: https://www.politesi.polimi.it/handle/10589/141225 (accessed on 26 June 2025).
38. Alimohammadi, V.; Maghfouri, M.; Nourmohammadi, D.; Azarsa, P.; Gupta, R.; Saberian, M. Stormwater runoff treatment using pervious concrete modified with various nanomaterials: A comprehensive review. *Sustainability* **2021**, *13*, 8552. [CrossRef]
39. İbiş, A.B. Investigation of Mechanical Properties of Porous Asphalt Pavement with Warm mix Asphalt Additive. Master's Thesis, Dokuz Eylul Universitesi, İzmir, Turkey, 2022.
40. Ćosić, K.; Korat, L.; Ducman, V.; Netinger, I. Influence of aggregate type and size on properties of pervious concrete. *Constr. Build. Mater.* **2015**, *78*, 69–76. [CrossRef]
41. Yu, F.; Sun, D.; Wang, J.; Hu, M. Influence of aggregate size on compressive strength of pervious concrete. *Constr. Build. Mater.* **2019**, *209*, 463–475. [CrossRef]
42. Sánchez-Mendieta, C.; Galán, J.J.; Martinez-Lage, I. Physical and hydraulic properties of porous concrete. *Sustainability* **2021**, *13*, 10562. [CrossRef]
43. Lamichhane, R.; Motra, G.B.; Khadka, T.B.; Zhang, Y.; Pathak, P.; Pandit, S. Impact of Water Level Variation on Mechanical Properties of Porous Concrete. *Sustainability* **2024**, *16*, 3546. [CrossRef]
44. Anburuvel, A.; Niruban Subramaniam, D. Investigation of the effects of compaction on compressive strength and porosity characteristics of pervious concrete. *Transp. Res. Rec.* **2022**, *2676*, 513–525. [CrossRef]
45. Li, L.G.; Feng, J.-J.; Xiao, B.-F.; Chu, S.-H.; Kwan, A.K.H. Roles of mortar volume in porosity, permeability and strength of pervious concrete. *J. Infrastruct. Preserv. Resil.* **2021**, *2*, 1–16.
46. Subramaniam, D.N.; Anburuvel, A. Performance Analysis Relevant to Primary Design Parameters of Pervious Concrete: A Critical Review. *Transp. Res. Rec.* **2024**, *2679*, 03611981241265851. [CrossRef]
47. Li, J.; Xia, J.; Di Sarno, L.; Gong, G. Fiber utilization in pervious concrete: Review on manufacture and properties. *Constr. Build. Mater.* **2023**, *406*, 133372. [CrossRef]
48. Neithalath, N.; Sumanasooriya, M.S.; Deo, O. Characterizing pore volume, sizes, and connectivity in pervious concretes for permeability prediction. *Mater. Charact.* **2010**, *61*, 802–813. [CrossRef]
49. Ahmad, S.; Azad, A.; Loughlin, K. A study of permeability and tortuosity of concrete. In Proceedings of the 30th Conference on Our World in Concrete and Structures, Singapore, 23–24 August 2005; pp. 23–24.
50. AlShareedah, O.; Nassiri, S. Spherical discrete element model for estimating the hydraulic conductivity and pore clogging of pervious concrete. *Constr. Build. Mater.* **2021**, *305*, 124749. [CrossRef]
51. Ning, J.; Huang, M.; Yu, J. Modelling of slurry infiltration in saturated porous media integrating particle dispersion and blockage. *Comput. Geotech.* **2025**, *177*, 106875. [CrossRef]
52. Fabbri, H.A.; Cleto, P.R.; Gaiotto, A.T., Jr.; Rodrigues, E.A.; Maedo, M.A.; Manzoli, O.L. Modeling the closure behavior of natural fractures in porous media using high aspect ratio interface elements. *J. Pet. Sci. Eng.* **2021**, *196*, 107979. [CrossRef]
53. Elsanoose, A.; Abobaker, E.; Khan, F.; Rahman, M.A.; Aborig, A.; Butt, S.D. Estimating of non-Darcy flow coefficient in artificial porous media. *Energies* **2022**, *15*, 1197. [CrossRef]
54. Neithalath, N.; Weiss, J.; Olek, J. Characterizing Enhanced Porosity Concrete using electrical impedance to predict acoustic and hydraulic performance. *Cem. Concr. Res.* **2006**, *36*, 2074–2085. [CrossRef]
55. Al-Jabari, M. 2-Concrete porosity and transport processes. In *Integral Waterproofing of Concrete Structures*; Woodhead Publishing: Cambridge, UK, 2022; pp. 37–68.
56. Mahdi, S.N.; Kolambekodi, K.; Arul, R.; Kataware, A.V.; Nawaukkaratharnant, N.; Nagaratnam, B. Optimizing Aggregate Selection and Mineral Additive to Enhance the Elasto-Mechanical Aspects of High-Performance Concrete. *Eng. Sci.* **2024**, *31*, 1270. [CrossRef]
57. Vasconcellos, A.T.D.; Matos, P.R.D.; Casagrande, C.A.; Ribeiro, A.V.S.; Prudêncio, L.R., Jr. Evaluating the variability of the modulus of elasticity of concrete through the use of different types and batches of aggregate. *Matéria* **2022**, *26*, e13117. [CrossRef]
58. Farahani, A.; Sharifi, M.; Bayesteh, H. Effect of aggregate size on the slump and uniaxial compressive strength of concrete: A DEM study. *Part. Sci. Technol.* **2025**, *43*, 15–32. [CrossRef]
59. Lee, M.-G.; Wang, W.-C.; Wang, Y.-C.; Hsieh, Y.-C.; Lin, Y.-C. Mechanical properties of high-strength pervious concrete with steel fiber or glass fiber. *Buildings* **2022**, *12*, 620. [CrossRef]
60. Jiang, Y.; Li, B.; Liu, S.; He, J.; Hernandez, A.G. Role of recycled concrete powder as sand replacement in the properties of cement mortar. *J. Clean. Prod.* **2022**, *371*, 133424. [CrossRef]
61. Oluokun, F.A.; Burdette, E.G.; Deatherage, J.H. Elastic modulus, Poisson's ratio, and compressive strength relationships at early ages. *Mater. J.* **1991**, *88*, 3–10.
62. Cetin, A.; Carrasquillo, R.L. High-performance concrete: Influence of coarse aggregates on mechanical properties. *ACI Mater. J.* **1998**, *95*, 252–261.

63. Haselbach, L.; Alam, A. Estimating the modulus of elasticity of pervious concrete based on porosity. *Adv. Civ. Eng. Mater.* **2014**, *3*, 256–269.
64. Gao, Y.; Jing, H.; Yu, Z.; Li, L.; Wu, J.; Chen, W. Particle size distribution of aggregate effects on the reinforcing roles of carbon nanotubes in enhancing concrete ITZ. *Constr. Build. Mater.* **2022**, *327*, 126964. [CrossRef]
65. de Araujo Thomaz, W.; Miyaji, D.Y.; Possan, E. Comparative study of dynamic and static Young's modulus of concrete containing basaltic aggregates. *Case Stud. Constr. Mater.* **2021**, *15*, e00645.
66. Tahir, M.F.M.; Abdullah, M.M.A.B.; Abd Rahim, S.Z.; Hasan, M.R.M.; Saafi, M.; Jaya, R.P.; Mohamed, R. Potential of industrial By-Products based geopolymer for rigid concrete pavement application. *Constr. Build. Mater.* **2022**, *344*, 128190. [CrossRef]
67. Tunçer, E. Sustainable Rubberized Pervious Concrete. Master's Thesis, Middle East Technical University, Ankara, Turkey, 2023.
68. Wijekoon, S.H.; Shajeefpiranath, T.; Subramaniam, D.N.; Sathiparan, N. A mathematical model to predict the porosity and compressive strength of pervious concrete based on the aggregate size, aggregate-to-cement ratio and compaction effort. *Asian J. Civ. Eng.* **2024**, *25*, 67–79. [CrossRef]
69. Zhang, W.-l.; Yuan, Z.-j.; Li, D.-Q.; Zhang, K.; Zhao, L.-Y. Mechanical and vegetation performance of porous concrete with recycled aggregate in riparian buffer area. *J. Clean. Prod.* **2022**, *332*, 130015. [CrossRef]
70. Zhang, Y.; Li, H.; Abdelhady, A.; Yang, J.; Wang, H. Effects of specimen shape and size on the permeability and mechanical properties of porous concrete. *Constr. Build. Mater.* **2021**, *266*, 121074. [CrossRef]
71. Sathiparan, N.; Wijekoon, S.H.; Ravi, R.; Jeyananthan, P.; Subramaniam, D.N. Response surface regression and machine learning models to predict the porosity and compressive strength of pervious concrete based on mix design parameters. *Road Mater. Pavement Des.* **2024**, *26*, 618–657. [CrossRef]
72. Muda, M.M.; Legese, A.M.; Urgessa, G.; Boja, T. Strength, porosity and permeability properties of porous concrete made from recycled concrete aggregates. *Constr. Mater.* **2023**, *3*, 81–92. [CrossRef]
73. Barua, G.; Islam, G.S. Low tortuous permeable concrete pavement material: A new approach to improve physical properties. *Clean. Eng. Technol.* **2024**, *20*, 100750. [CrossRef]
74. Elizondo-Martínez, E.J.; Andrés-Valeri, V.C.; Juli-Gándara, L.; Rodriguez-Hernandez, J. Multi-criteria optimum mixture design of porous concrete pavement surface layers. *Int. J. Pavement Eng.* **2022**, *23*, 745–754. [CrossRef]
75. Li, T.; Tang, X.; Xia, J.; Gong, G.; Xu, Y.; Li, M. Investigation of mechanical strength, permeability, durability and environmental effects of pervious concrete from travertine waste material. *Constr. Build. Mater.* **2024**, *426*, 136175. [CrossRef]
76. Fan, S.; Ren, H.; Hong, S.; Xing, F.; Hou, D.; Dong, B. Interfacial mechanical bond characterization between cement pastes and porous aggregates through a coupled XCT and DVC technique. *Cem. Concr. Compos.* **2023**, *142*, 105158. [CrossRef]
77. Zhong, R.; Wille, K. Compression response of normal and high strength pervious concrete. *Constr. Build. Mater.* **2016**, *109*, 177–187. [CrossRef]
78. Ozel, B.F.; Sakallı, Ş.; Gündüz, Y.; Şahin, Y. Freeze–thaw resistance of pervious concrete produced with different aggregates and fibres. *Road Mater. Pavement Des.* **2024**, 1–23. [CrossRef]
79. Yang, J.; Jiang, G. Experimental study on properties of pervious concrete pavement materials. *Cem. Concr. Res.* **2003**, *33*, 381–386. [CrossRef]
80. Montes, F.; Valavala, S.; Haselbach, L.M. A new test method for porosity measurements of Portland cement pervious concrete. *J. ASTM Int.* **2005**, *2*, 1–13. [CrossRef]
81. Yavuz, D.; Yazıcı, Ş.; Avcı, M.S.; Özmen, D. A novel approach to estimate the tortuosity of pervious concretes using computed tomography. *Mater. Struct.* **2023**, *56*, 74. [CrossRef]
82. Yaghmour, E.; Yan, L.; Naito, C.; Suleiman, M.; Fox, J.; Romero, C.; Neti, S. Energy storage in lightweight aggregate and pervious concrete infused with phase change materials. *Appl. Therm. Eng.* **2024**, *250*, 123430. [CrossRef]
83. Kalman, H.; Portnikov, D. Analyzing bulk density and void fraction: A. the effect of archimedes number. *Powder Technol.* **2021**, *381*, 477–487. [CrossRef]
84. *ASTM C173*; Content, Air Volumetric Method for Lightweight or Normal Weight Concrete. ASTM C: Conshohocken, PA, USA, 2014; p. 231.
85. Neville, A.M. *Properties of Concrete*, 4th ed.; Addison Wesley Longman Ltd.: Essex, UK, 1995.
86. He, S.; Chen, Y.; Liang, M.; Yang, E.-H.; Schlangen, E. Distribution of porosity surrounding a microfiber in cement paste. *Cem. Concr. Compos.* **2023**, *142*, 105188. [CrossRef]
87. Yavuz, D.; Akbulut, Z.F.; Guler, S. Porous concrete modification with silica fume and ground granulated blast furnace slag: Hydraulic and mechanical properties before and after freeze-thaw exposure. *Constr. Build. Mater.* **2024**, *447*, 138099. [CrossRef]
88. Ibrahim, A.; Mahmoud, E.; Yamin, M.; Patibandla, V.C. Experimental study on Portland cement pervious concrete mechanical and hydrological properties. *Constr. Build. Mater.* **2014**, *50*, 524–529. [CrossRef]
89. Sumanasooriya, M.S.; Neithalath, N. Pore structure features of pervious concretes proportioned for desired porosities and their performance prediction. *Cem. Concr. Compos.* **2011**, *33*, 778–787. [CrossRef]

90. Lim, E.; Tan, K.H.; Fwa, T.F. High-strength high-porosity pervious concrete pavement. In *Advanced Materials Research*; Trans Tech Publ: Zürich, Switzerland, 2013; pp. 361–367.
91. Putra Jaya, R.; Yusak, M.; IBRAHIM, M.; Hainin, M. A Review of Porous Concrete Pavement: Applications and Engineering Properties. *Appl. Mech. Mater.* **2014**, *554*, 37–41.
92. Su, X.; Ren, Z.; Li, P. Review on physical and chemical activation strategies for ultra-high performance concrete (UHPC). *Cem. Concr. Compos.* **2024**, *149*, 105519. [CrossRef]
93. Lu, Z.; Lu, J.; Liu, Z.; Sun, Z.; Stephan, D. Influence of water to cement ratio on the compatibility of polycarboxylate superplasticizer with Portland cement. *Constr. Build. Mater.* **2022**, *341*, 127846. [CrossRef]
94. Xie, Z.; Tian, Y.; Li, Y.; Hu, J.; Jamaa, G.M.; Yuan, Q.; Zhu, X. Understanding the temperature-dependent workability of cement paste with polycarboxylate superplasticizer. *J. Build. Eng.* **2023**, *76*, 107408. [CrossRef]
95. Nguyen, T.T. Experimental investigation and numerical modeling on mechanical behavior of highly porous cement-based material: An overview. *Mech. Adv. Mater. Struct.* **2024**, *31*, 9040–9061. [CrossRef]
96. Şahin, H.G.; Mardani, A.; Beytekin, H.E. Effect of silica fume utilization on structural build-up, mechanical and dimensional stability performance of fiber-reinforced 3D printable concrete. *Polymers* **2024**, *16*, 556. [CrossRef]
97. AlTawaiha, H.; Alhomaidat, F.; Eljufout, T. A review of the effect of nano-silica on the mechanical and durability properties of cementitious composites. *Infrastructures* **2023**, *8*, 132. [CrossRef]
98. Shtrepi, L.; Astolfi, A.; Badino, E.; Volpatti, G.; Zampini, D. More than just concrete: Acoustically efficient porous concrete with different aggregate shape and gradation. *Appl. Sci.* **2021**, *11*, 4835. [CrossRef]
99. Vishalakshi, K.; Revathi, V.; Reddy, S.S. Effect of type of coarse aggregate on the strength properties and fracture energy of normal and high strength concrete. *Eng. Fract. Mech.* **2018**, *194*, 52–60. [CrossRef]
100. Lan, X.; Zhang, X.; Hao, Z.; Wang, Y. Strength and shrinkage properties of cement stabilized macadam bases incorporating 0–2.36 millimetre recycled fine aggregate. *Case Stud. Constr. Mater.* **2022**, *16*, e00984. [CrossRef]
101. Daniel, T.T. Examination on the Influence of Aggregate Size and Gradation on Porous Concrete Performance. Ph.D. Thesis, Bahir Dar University, Bahir Dar, Ethiopia, 2020.
102. Huang, W.; Cai, X.; Li, X.; Cui, W.; Wu, K. Influence of nominal maximum aggregate size and aggregate gradation on pore characteristics of porous asphalt concrete. *Materials* **2020**, *13*, 1355. [CrossRef] [PubMed]
103. Elmagarhe, A.; Lu, Q.; Alamri, M.; Alharthai, M.; Elnihum, A. Laboratory performance evaluation of porous asphalt mixture containing recycled concrete aggregate and fly ash. *Case Stud. Constr. Mater.* **2024**, *20*, e02849. [CrossRef]
104. Smirnov, D.; Stepanov, S.; Garipov, R.; Garayev, T.; Sungatullin, T. Influence of the porosity structure of road concrete on its durability. In *E3S Web of Conferences*; EDP Sciences: Paris, France, 2021; p. 04009.
105. Darshan, N.; Kataware, A.V. Review on porous asphalt pavements: A comprehensive resolution for Stormwater management and applications in current built environment. *Int. J. Pavement Res. Technol.* **2024**, 1–25. [CrossRef]
106. Małgorzata, F. *Application of Waste Materials in Lightweight Aggregates*; Taylor & Francis: Oxfordshire, UK, 2023.
107. Sandoval, G.F.; Pieralisi, R.; de Souza Risson, K.D.B.; de Moura, A.C.; Toralles, B.M. Clogging phenomenon in Pervious Concrete (PC): A systematic literature review. *J. Clean. Prod.* **2022**, *365*, 132579. [CrossRef]
108. Wu, S.; Wu, Q.; Shan, J.; Cai, X.; Su, X.; Sun, X. Effect of morphological characteristics of aggregate on the performance of pervious concrete. *Constr. Build. Mater.* **2023**, *367*, 130219. [CrossRef]
109. Zhou, S.; Wu, C.; Li, J.; Shi, Y.; Wang, Y.; Luo, M. The Impact of Coarse Aggregate Parent Rock Types on the Freeze–Thaw Resistance of Hydraulic Concrete. *Buildings* **2023**, *15*, 977. [CrossRef]
110. Kevern, J.T.; Wang, K.; Schaefer, V.R. Effect of coarse aggregate on the freeze-thaw durability of pervious concrete. *J. Mater. Civ. Eng.* **2009**, *22*, 469–475. [CrossRef]
111. ACI Committee 522. *Report on Pervious Concrete*; ACI 522R-10; American Concrete Institute: Farmington Hills, MI, USA, 2010.
112. Nguyen, D.H.; Sebaibi, N.; Boutouil, M.; Leleyter, L.; Baraud, F. A modified method for the design of pervious concrete mix. *Constr. Build. Mater.* **2014**, *73*, 271–282. [CrossRef]
113. Yahia, A.; Kabagire, K.D. New approach to proportion pervious concrete. *Constr. Build. Mater.* **2014**, *62*, 38–46. [CrossRef]
114. Marathe, S.; Sadowski, Ł.; Shree, N. Geopolymer and alkali-activated permeable concrete pavements: Bibliometrics and systematic current state of the art review, applications, and perspectives. *Constr. Build. Mater.* **2024**, *421*, 135586. [CrossRef]
115. Sathiparan, N.; Jeyananthan, P.; Subramaniam, D.N. A machine learning approach to predicting pervious concrete properties: A review. *Innov. Infrastruct. Solut.* **2025**, *10*, 55. [CrossRef]
116. Niyomukiza, J.B.; Eisazadeh, A.; Tangtermsirikul, S. Recent advances in slope stabilization using porous vegetation concrete in landslide-prone regions: A review. *J. Build. Eng.* **2023**, *76*, 107129. [CrossRef]
117. Chu, A.S. Volume-Based Concrete Mixture Design. *ACI Mater. J.* **2023**, *120*, 243.
118. Ghafoori, N.; Dutta, S. Laboratory investigation of compacted no-fines concrete for paving materials. *J. Mater. Civ. Eng.* **1995**, *7*, 183–191. [CrossRef]

119. Crouch, L.; Pitt, J.; Hewitt, R. Aggregate effects on pervious Portland cement concrete static modulus of elasticity. *J. Mater. Civ. Eng.* **2007**, *19*, 561–568. [CrossRef]
120. Huang, B.; Wu, H.; Shu, X.; Burdette, E.G. Laboratory evaluation of permeability and strength of polymer-modified pervious concrete. *Constr. Build. Mater.* **2010**, *24*, 818–823. [CrossRef]
121. Lim, E.; Tan, K.H.; Fwa, T.F. Effect of mix proportion on strength and permeability of pervious concrete for use in pavement. *J. East. Asia Soc. Transp. Stud.* **2013**, *10*, 1565–1575.
122. Wang, Z.; Zou, D.; Liu, T.; Zhou, A. Influence of paste coating thickness on the compressive strength, permeability, and mesostructure of permeable concrete. *Constr. Build. Mater.* **2021**, *299*, 123994. [CrossRef]
123. Rao, Y.; Yang, T.; Chen, H.; Wu, Y.; Li, H.; Wang, H. Comparison of gravimetric methods to measure regional porosity distribution in porous concrete pavement. *Road Mater. Pavement Des.* **2023**, *24*, 866–879. [CrossRef]
124. Ghanbari, M.; Moghaddam, F.E.; Shayeganfar, F.; Beheshtian, J.; Sanayei, A.; Ramazani, A. Cement based nanofiltration membrane of porous boron nitride and graphene oxide for effective oil/water separation. *J. Mol. Liq.* **2024**, *408*, 125268. [CrossRef]
125. Azad, A.; Mousavi, S.-F.; Karami, H.; Farzin, S.; Singh, V.P. The effect of vermiculite and quartz in porous concrete on reducing storm-runoff pollution. *ISH J. Hydraul. Eng.* **2021**, *27*, 144–152. [CrossRef]
126. Kewalramani, M.; Khartabil, A. Porosity evaluation of concrete containing supplementary cementitious materials for durability assessment through volume of permeable voids and water immersion conditions. *Buildings* **2021**, *11*, 378. [CrossRef]
127. Marshdi, Q.S.R.; Hussien, S.A.; Mareai, B.M.; Al-Khafaji, Z.S.; Shubbar, A. Applying of No-fines concretes as a porous concrete in different construction application. *Period. Eng. Nat. Sci. (PEN)* **2021**, *9*, 999–1012. [CrossRef]
128. Zvonarić, M.; Barišić, I.; Galić, M.; Minažek, K. Influence of laboratory compaction method on compaction and strength characteristics of unbound and cement-bound mixtures. *Appl. Sci.* **2021**, *11*, 4750. [CrossRef]
129. Merino-Lechuga, A.M.; Lamaa, G.; Silva, R.V.; de Brito, J.; Jiménez, J.R.; Fernández-Rodríguez, J.M.; González-Caro, Á. Accelerated carbonation of alkali-activated vibro-compacted pervious concrete paving blocks. *Constr. Build. Mater.* **2024**, *449*, 138458. [CrossRef]
130. Avudaiappan, S.; Amran, M.; Aepuru, R.; Fediuk, R.; Vatin, N. Prediction of pore volume dispersion and microstructural characteristics of concrete using image processing technique. *Crystals* **2021**, *11*, 1476. [CrossRef]
131. Sajeevan, M.; Subramaniam, D. Investigation of boundary layer impact on pervious concrete. *Int. J. Pavement Eng.* **2023**, *24*, 2111423. [CrossRef]
132. Bustillo Revuelta, M.; Bustillo Revuelta, M. Concrete. In *Construction Materials: Geology, Production and Applications*; Springer Nature: Berlin/Heidelberg, Germany, 2021; pp. 217–274.
133. Jia, H.; Yang, X.; Wei, Y.; Sun, Q.; Tang, L. Capillary Imbibition Laws of Fresh–Brackish Waters in Sandstone. *Water* **2024**, *16*, 1180. [CrossRef]
134. Wang, Y.; Jia, Y.; Tang, L.; Wen, J.; Zhan, Q.; Wang, Y. Experimental study on aerial detection of concrete microcracks based on fluorescent selective excitation. *Nondestruct. Test. Eval.* **2024**, *40*, 988–1015. [CrossRef]
135. Praticò, F.; Fedele, R.; Briante, P. On the Dependence of Acoustic Pore Shape Factors on Porous Asphalt Volumetrics. *Sustainability* **2021**, *13*, 11541. [CrossRef]
136. Kabir, T.; Al-Bayati, H.K.; Tighe, S. Laboratory mix preparation and investigation of mechanical behaviour of polyurethane-bound porous rubber pavement. *Can. J. Civ. Eng.* **2024**, *51*, 1350–1368. [CrossRef]
137. Zhu, J.; Ma, T.; Lin, Z.; Xu, J.; Qiu, X. Evaluation of internal pore structure of porous asphalt concrete based on laboratory testing and discrete-element modeling. *Constr. Build. Mater.* **2021**, *273*, 121754. [CrossRef]
138. Muzyka, R.; Misztal, E.; Hrabak, J.; Banks, S.W.; Sajdak, M. Various biomass pyrolysis conditions influence the porosity and pore size distribution of biochar. *Energy* **2023**, *263*, 126128. [CrossRef]
139. Ma, R.; Jiang, Y.; Liu, B.; Fan, H. Effects of pore structure characterized by synchrotron-based micro-computed tomography on aggregate stability of black soil under freeze-thaw cycles. *Soil Tillage Res.* **2021**, *207*, 104855. [CrossRef]
140. Li, L.G.; Feng, J.-J.; Zhu, J.; Chu, S.-H.; Kwan, A.K.H. Pervious concrete: Effects of porosity on permeability and strength. *Mag. Concr. Res.* **2021**, *73*, 69–79. [CrossRef]
141. Safiuddin, M.; Hearn, N. Comparison of ASTM saturation techniques for measuring the permeable porosity of concrete. *Cem. Concr. Res.* **2005**, *35*, 1008–1013. [CrossRef]
142. Matsuo, Y.; Morino, K.; Iwatsuki, E. A study of porous concrete using electric arc furnace oxidizing slag aggregate. *Bull. Aichi Inst. Technology. Part B* **2005**, *40*, 167–217.
143. Bentz, D.P. Virtual pervious concrete: Microstructure, percolation, and permeability. *ACI Mater. J.* **2008**, *105*, 297.
144. Yang, J.; Mahato, J.; Moon, J. Effects of various sizes of cenospheres on microstructural, mechanical, and thermal properties of high-strength and lightweight cementitious composites. *J. Build. Eng.* **2023**, *76*, 107214. [CrossRef]
145. Sansalone, J.; Kuang, X.; Ranieri, V. Permeable pavement as a hydraulic and filtration interface for urban drainage. *J. Irrig. Drain. Eng.* **2008**, *134*, 666–674. [CrossRef]

146. Sumanasooriya, M.S.; Neithalath, N. Stereology-and Morphology-Based Pore Structure Descriptors of Enhanced Porosity (Pervious) Concretes. *ACI Mater. J.* **2009**, *106*, 210–217.
147. Haselbach, L.M.; Freeman, R.M. Vertical porosity distributions in pervious concrete pavement. *ACI Mater. J.* **2006**, *103*, 452–458.
148. Martin, W.D., III; Putman, B.J.; Kaye, N.B. Using image analysis to measure the porosity distribution of a porous pavement. *Constr. Build. Mater.* **2013**, *48*, 210–217. [CrossRef]
149. Huang, J.; Zhang, Y.; Sun, Y.; Ren, J.; Zhao, Z.; Zhang, J. Evaluation of pore size distribution and permeability reduction behavior in pervious concrete. *Constr. Build. Mater.* **2021**, *290*, 123228. [CrossRef]
150. Shan, J.; Zhang, Y.; Wu, S.; Lin, Z.; Li, L.; Wu, Q. Pore characteristics of pervious concrete and their influence on permeability attributes. *Constr. Build. Mater.* **2022**, *327*, 126874. [CrossRef]
151. De Somer, M.; De Winne, E.; AIPCR. Method to establish the'porosity-depth'distribution of porous concrete pavement using cylindrical 100 cm2 cores samples. In Proceedings of the 8th International Symposium on Concrete Roads, AIPCR, Lissabon, Portugal, 13–16 September 1998; pp. 171–176.
152. Lin, W.; Liu, L.; Ye, H.; Yu, Q.; Cho, Y.-H. Analyzing the Influence of Pore Structure and Vibration on Clogging in Pervious Concrete. *J. Clean. Prod.* **2025**, *495*, 145065. [CrossRef]
153. Abousnina, R. The Influence of Crude Oil Contamination on the Microstructure Properties of Fly Ash-Based Geopolymer Cement. In Proceedings of the ICSDI 2024, Riyadh, Saudi Arabia, 18–22 February 2024; Mansour, Y., Subramaniam, U., Mustaffa, Z., Abdelhadi, A., Ezzat, M., Abowardah, E., Eds.; Springer Nature: Singapore, 2025; Volume 1, pp. 357–364.
154. Abousnina, R.M.B. Properties of Mortar and Concrete Containing Fine Sand Contaminated with Light Crude Oil. Ph.D. Thesis, University of Southern Queensland, Toowoomba, Australia, 2016.
155. Fu, J.; Thomas, H.R.; Li, C. Tortuosity of porous media: Image analysis and physical simulation. *Earth-Sci. Rev.* **2021**, *212*, 103439. [CrossRef]
156. de Oliveira, J.A.; Cássaro, F.A.; Pires, L.F. Estimating soil porosity and pore size distribution changes due to wetting-drying cycles by morphometric image analysis. *Soil Tillage Res.* **2021**, *205*, 104814. [CrossRef]
157. Schaefer, V.R.; Wang, K.; Suleiman, M.T.; Kevern, J.T. *Mix Design Development for Pervious Concrete in Cold Weather Climates*; Rosap: Berlin, Germany, 2006.
158. Kevern, J.; Wang, K.; Suleiman, M.T.; Schaefer, V. Mix design development for pervious concrete in cold weather climates. In Proceedings of the Mid-Continent Transportation Research Symposium, Ames, IA, USA, 18–19 August 2005.
159. Park, S.-B.; Tia, M. An experimental study on the water-purification properties of porous concrete. *Cem. Concr. Res.* **2004**, *34*, 177–184. [CrossRef]
160. Maguesvari, M.U.; Narasimha, V.L. Studies on Characterization of Pervious Concrete for Pavement Applications. *Procedia—Soc. Behav. Sci.* **2013**, *104*, 198–207. [CrossRef]
161. Lian, C.; Zhuge, Y.; Beecham, S. The relationship between porosity and strength for porous concrete. *Constr. Build. Mater.* **2011**, *25*, 4294–4298. [CrossRef]
162. Chindaprasirt, P.; Hatanaka, S.; Mishima, N.; Yuasa, Y.; Chareerat, T. Effects of binder strength and aggregate size on the compressive strength and void ratio of porous concrete. *Int. J. Miner. Metall. Mater.* **2009**, *16*, 714–719.
163. Vijai, K.; Kumutha, R.; Vishnuram, B. Effect of types of curing on strength of geopolymer concrete. *Int. J. Phys. Sci.* **2010**, *5*, 1419–1423.
164. Tho-in, T.; Sata, V.; Chindaprasirt, P.; Jaturapitakkul, C. Pervious high-calcium fly ash geopolymer concrete. *Constr. Build. Mater.* **2012**, *30*, 366–371. [CrossRef]
165. Aoki, Y. *Development of Pervious Concrete*; University of Technology Sydney: Ultimo, Australia, 2010.
166. He, S.-S.; Jiao, C.-J.; Li, S. Investigation of mechanical strength and permeability characteristics of pervious concrete mixed with coral aggregate and seawater. *Constr. Build. Mater.* **2023**, *363*, 129508. [CrossRef]
167. Wei, Y.; Chen, Z.; Yio, M.; Cheeseman, C.; Wang, H.; Poon, C.S. Advanced moisture control in porous aggregates for improved lightweight high-performance concrete. *Cem. Concr. Compos.* **2025**, *155*, 105826. [CrossRef]
168. Ferić, K.; Sathish Kumar, V.; Romić, A.; Gotovac, H. Effect of aggregate size and compaction on the strength and hydraulic properties of pervious concrete. *Sustainability* **2023**, *15*, 1146. [CrossRef]
169. Paula Junior, A.C.; Jacinto, C.; Oliveira, T.M.; Polisseni, A.E.; Brum, F.M.; Teixeira, E.R.; Mateus, R. Characterisation and life cycle assessment of pervious concrete with recycled concrete aggregates. *Crystals* **2021**, *11*, 209. [CrossRef]
170. Guan, H.; Yu, J.; Umuhuza Kibugenza, A.S.; Sun, Q. Preparation of coal gangue ceramsite high-strength concrete and investigation of its physico-mechanical properties. *Sci. Rep.* **2022**, *12*, 16369. [CrossRef]
171. Bandyopadhyay, A.; Mitra, I.; Avila, J.D.; Upadhyayula, M.; Bose, S. Porous metal implants: Processing, properties, and challenges. *Int. J. Extrem. Manuf.* **2023**, *5*, 032014. [CrossRef] [PubMed]
172. Zouaghi, A.; Nakazawa, T.; IMAI, F.; Shinnishi, N. Permeability of no-fines concrete. *Trans. Jpn. Concr. Inst.* **1999**, *20*, 31–38.
173. Tennis, P.D.; Leming, M.L.; Akers, D.J. *Pervious Concrete Pavements*; no. PCA Serial No. 2828; Portland Cement Association: Skokie, IL, USA, 2004.

174. Zhuge, Y. *A Review of Permeable Concrete and Its Application to Pavements*; Taylor & Francis Group: Oxfordshire, UK, 2006.
175. Tsivilis, S.; Tsantilas, J.; Kakali, G.; Chaniotakis, E.; Sakellariou, A. The permeability of Portland limestone cement concrete. *Cem. Concr. Res.* **2003**, *33*, 1465–1471. [CrossRef]
176. Gorninski, J.P.; Dal Molin, D.C.; Kazmierczak, C.S. Study of the modulus of elasticity of polymer concrete compounds and comparative assessment of polymer concrete and portland cement concrete. *Cem. Concr. Res.* **2004**, *34*, 2091–2095. [CrossRef]
177. Liu, C.; Xia, Y.; Chen, J.; Huang, K.; Wang, J.; Wang, C.; Huang, Z.; Wang, X.; Rao, C.; Shi, M. Research and application progress of vegetation porous concrete. *Materials* **2023**, *16*, 7039. [CrossRef] [PubMed]
178. Zhu, S.-W.; Jiao, C.-J.; Li, H.-Y.; Chen, X.-F. Mathematical modeling of mechanical and physical properties of ecological pervious concrete containing recycled aggregates. *J. Build. Eng.* **2024**, *92*, 109681. [CrossRef]
179. Yu, Z.; Gan, H.; Xiao, M.; Huang, B.; Zhu, D.Z.; Zhang, Z.; Wang, H.; Lin, Y.; Hou, Y.; Peng, S. Performance of permeable pavement systems on stormwater permeability and pollutant removal. *Environ. Sci. Pollut. Res.* **2021**, *28*, 28571–28584. [CrossRef]
180. Abduljaleel, Y.; Chikabvumbwa, S.R.; Haq, F.U. Assessing the efficacy of Permeable Interlocking Concrete Pavers (PICP) in managing stormwater runoff under climate change and land use scenarios. *J. Hydrol.* **2025**, *646*, 132329. [CrossRef]
181. Lv, H.; Xiong, Z.; Li, H.; Liu, J.; Xu, G.; Chen, H. Investigating the Mechanical Properties and Water Permeability of Recycled Pervious Concrete Using Three Typical Gradation Schemes. *Buildings* **2025**, *15*, 358. [CrossRef]
182. Sandoval, G.F.; Pieralisi, R. Sustainable aggregate impact on pervious concrete abrasion resistance. *Results Eng.* **2023**, *20*, 101384. [CrossRef]
183. Huang, K.-L.; Song, Y.; Sheng, Y.-M. Rainstorm Resistance of Recycled Pervious Concrete under the Coupling of Fatigue and Freeze–Thaw Cycles. *Buildings* **2024**, *14*, 294. [CrossRef]
184. Fujiwara, H.; Tomita, R.; Okamoto, T.; Dozono, A.; Obatake, A. Properties of high-strength porous concrete. *Buildings* **1998**, *14*, 294.
185. Martin, W.D.; Kaye, N.B.; Putman, B.J. Impact of vertical porosity distribution on the permeability of pervious concrete. *Constr. Build. Mater.* **2014**, *59*, 78–84. [CrossRef]
186. Martin, W. Hydraulic Impact of Porosity Distribution and Hydrologic Characterization of Porous Pavements. Ph.D. Thesis, Clemson University, Clemson, SC, USA, 2013.
187. Badoe, D.A.; Honeycutt, K.R.; Crouch, L.; Cates, M.A.; Dotson, V.J. Measuring the effective air void content of Portland cement pervious pavements. *Cem. Concr. Aggreg.* **2003**, *25*, 1–5.
188. Bradford, S.A.; Bettahar, M.; Simunek, J.; Van Genuchten, M.T. Straining and attachment of colloids in physically heterogeneous porous media. *Vadose Zone J.* **2004**, *3*, 384–394. [CrossRef]
189. Haselbach, L.M.; Freeman, R.M. Effectively estimating in situ porosity of pervious concrete from cores. *J. ASTM Int.* **2007**, *4*, JAI100293. [CrossRef]
190. Abousnina, R.M.; Manalo, A.; Lokuge, W. Physical and Mechanical Properties of Cement Mortar Containing Fine Sand Contaminated with Light Crude Oil. *Procedia Eng.* **2016**, *145*, 250–258. [CrossRef]
191. Xu, G.; Shen, W.; Huo, X.; Yang, Z.; Wang, J.; Zhang, W.; Ji, X. Investigation on the properties of porous concrete as road base material. *Constr. Build. Mater.* **2018**, *158*, 141–148. [CrossRef]
192. Seifeddine, K.; Amziane, S.; Toussaint, E. State of the art on the mechanical properties of pervious concrete. *Eur. J. Environ. Civ. Eng.* **2022**, *26*, 7727–7755. [CrossRef]
193. Thibault, B.; Aghajanzadeh, S.; Sultana, A.; Ratti, C.; Khalloufi, S. Characteristics of Open and Closed Pores, Their Measurement Techniques and Exploitation in Dehydrated Food Products. *Food Eng. Rev.* **2024**, *16*, 323–355. [CrossRef]
194. Haider, M.Z.; Jin, X.; Naqvi, S.N.R.; Hu, J.W. Enhanced snow melting efficiency in thermal energy storage concrete incorporated with carbon nanotubes for pavement applications. *J. Energy Storage* **2025**, *107*, 114937. [CrossRef]
195. Naylor, D.; Tsai, S.S.H. Archimedes' principle with surface tension effects in undergraduate fluid mechanics. *Int. J. Mech. Eng. Educ.* **2022**, *50*, 749–763. [CrossRef]
196. Jaques, V.A.J.; Plessis, A.D.; Zemek, M.; Šalplachta, J.; Stubianová, Z.; Zikmund, T.; Kaiser, J. Review of porosity uncertainty estimation methods in computed tomography dataset. *Meas. Sci. Technol.* **2021**, *32*, 122001. [CrossRef]
197. Xiao, N.; Berto, F.; Zhou, X. Three-dimensional stochastic reconstruction of porous media: A systematic review. *J. Build. Eng.* **2024**, *91*, 109642. [CrossRef]
198. Nooraiepour, M.; Masoudi, M.; Shokri, N.; Hellevang, H. Probabilistic Nucleation and Crystal Growth in Porous Medium: New Insights from Calcium Carbonate Precipitation on Primary and Secondary Substrates. *ACS Omega* **2021**, *6*, 28072–28083. [CrossRef]
199. Ling, S.; Sun, Y.; Sun, D.; Jelagin, D. Pore characteristics and permeability simulation of porous asphalt mixture in pouring semi-flexible pavement. *Constr. Build. Mater.* **2022**, *330*, 127253. [CrossRef]
200. Ma, X.; Jiang, J.; Zhao, Y.; Wang, H. Characterization of the interconnected pore and its relationship to the directional permeability of porous asphalt mixture. *Constr. Build. Mater.* **2021**, *269*, 121233. [CrossRef]

201. Ni, T.; Ma, W.; Yang, Y.; Yu, J.; Liu, J.; Jiang, C.; Gu, C. Interface reinforcement and a new characterization method for pore structure of pervious concrete. *Constr. Build. Mater.* **2021**, *267*, 121052. [CrossRef]
202. Safari, H.; Balcom, B.J.; Afrough, A. Characterization of pore and grain size distributions in porous geological samples—An image processing workflow. *Comput. Geosci.* **2021**, *156*, 104895. [CrossRef]
203. Rabbani, A.; Fernando, A.M.; Shams, R.; Singh, A.; Mostaghimi, P.; Babaei, M. Review of Data Science Trends and Issues in Porous Media Research With a Focus on Image-Based Techniques. *Water Resour. Res.* **2021**, *57*, e2020WR029472. [CrossRef]
204. Yang, Z. Freezing-and-Thawing Durability of Pervious Concrete under Simulated Field Conditions. *ACI Mater. J.* **2011**, *108*, 187–195.
205. Wijeyawardana, P.; Nanayakkara, N.; Gunasekara, C.; Karunarathna, A.; Law, D.; Pramanik, B.K. Improvement of heavy metal removal from urban runoff using modified pervious concrete. *Sci. Total Environ.* **2022**, *815*, 152936. [CrossRef]
206. Saghaian Nejad, S.; Abedi-Koupai, J.; Mostafazadeh-Fard, S.; Behfarnia, K. Treatment of urban storm water using adsorbent porous concrete. *Proc. Inst. Civ. Eng.—Water Manag.* **2018**, *171*, 328–334. [CrossRef]
207. Mikhailenko, P.; Piao, Z.; Kakar, M.R.; Bueno, M.; Athari, S.; Pieren, R.; Heutschi, K.; Poulikakos, L. Low-Noise pavement technologies and evaluation techniques: A literature review. *Int. J. Pavement Eng.* **2022**, *23*, 1911–1934. [CrossRef]
208. Osuji, S.; Nwankwo, E. Effect of crude oil contamination on the compressive strength of concrete. *Niger. J. Technol.* **2015**, *34*, 259–265. [CrossRef]
209. Abousnina, R.; Manalo, A.; Lokuge, W.; Zhang, Z. Effects of light crude oil contamination on the physical and mechanical properties of geopolymer cement mortar. *Cem. Concr. Compos.* **2018**, *90*, 136–149. [CrossRef]
210. Wijekoon, S.H.B.; Sathiparan, N.; Subramaniam, D.N. Optimisation of pervious concrete performance by varying aggregate shape, size, aggregate-to-cement ratio, and compaction effort by using the Taguchi method. *Int. J. Pavement Eng.* **2024**, *25*, 2380523. [CrossRef]
211. Chandrappa, A.K.; Biligiri, K.P. Pervious concrete as a sustainable pavement material–Research findings and future prospects: A state-of-the-art review. *Constr. Build. Mater.* **2016**, *111*, 262–274. [CrossRef]
212. Li, H.; Kayhanian, M.; Harvey, J.T. Comparative field permeability measurement of permeable pavements using ASTM C1701 and NCAT permeameter methods. *J. Environ. Manag.* **2013**, *118*, 144–152. [CrossRef]
213. Abousnina, R.M.; Manalo, A.; Shiau, J.; Lokuge, W. Effects of Light Crude Oil Contamination on the Physical and Mechanical Properties of Fine Sand. *Soil Sediment Contam. Int. J.* **2015**, *24*, 833–845. [CrossRef]

Disclaimer/Publisher's Note: The statements, opinions and data contained in all publications are solely those of the individual author(s) and contributor(s) and not of MDPI and/or the editor(s). MDPI and/or the editor(s) disclaim responsibility for any injury to people or property resulting from any ideas, methods, instructions or products referred to in the content.